

# Source Regions of Coronal Mass Ejections

Prasad Subramanian<sup>1</sup>

Center for Earth Observing and Space Research, George Mason University, Fairfax, VA  
22030, USA

`psubrama@iucaa.ernet.in`

K. P. Dere October 27, 2018

Naval Research Laboratory, Code 7660, Washington, DC 20375, USA

`dere@halcyon.nrl.navy.mil`

Received \_\_\_\_\_; accepted \_\_\_\_\_

submitted to the Astrophysical Journal

---

<sup>1</sup>Present address: IUCAA, P.O Bag No: 4, Ganeshkhind, Pune 411007, India

## ABSTRACT

Observations of the solar corona with the Large Angle Spectrometric Coronagraph (LASCO) and Extreme ultraviolet Imaging Telescope (EIT) instruments on the Solar and Heliospheric Observatory (SOHO) provide an unprecedented opportunity to study coronal mass ejections (CMEs) from their initiation through their evolution out to  $30 R_{\odot}$ . The objective of this study is to gain an understanding of the source regions from which the CMEs emanate. To this end, we have developed a list of 32 CMEs whose source regions are located on the solar disk and are well observed in EIT 195 Å data during the period from solar minimum in January 1996 through the rising part of the cycle in May 1998. We compare the EIT source regions with photospheric magnetograms from the Michelson Doppler Imager (MDI) instrument on SOHO and the NSO/Kitt Peak Observatory and also with  $H\alpha$  data from various sources. The overall results of our study show that 41% of the CME related transients observed are associated with active regions and have no prominence eruptions, 44% are associated with eruptions of prominences embedded in active regions and 15% are associated with eruptions of prominences outside active regions. Those CMEs that do not involve prominence eruptions originate in active regions both with and without prominences. We describe 6 especially well observed events. These case studies suggest that active region CMEs (without eruptive prominences) are associated with active regions with lifetimes between 11–80 days. They are also often associated with small scale emerging or cancelling flux over timescales of 6–7 hours. CMEs associated with active region prominence eruptions, on the other hand, are typically associated with old active regions with lifetimes  $\sim$  6-7 months.

*Subject headings:* Sun: corona, prominences

## 1. Introduction

In this paper, we concentrate on CME source regions with a view to gaining insight into the initiation mechanism of CMEs, especially in relation to pre-existing coronal structures and the underlying photospheric magnetic field. We confine our attention to CMEs observed in LASCO white light images that have clearly identifiable on-disk counterparts in EIT 195 Å data that are well away from the solar limb. The photons detected by the EIT 195 Å channel are primarily due to Fe XII formed at a temperature around  $1.4 \times 10^6$  K (Dere et al. 2000).

We address such questions as:

1. What are the source regions of CMEs?
2. Are there any discernible characteristics of the source regions indicating an inclination for producing CMEs?
3. How are CMEs related to active regions and prominence eruptions?
4. What is the short and long-term temporal evolution of CME producing regions?

Several recent papers have reported on instances of phenomena in the lower corona in EIT 195 Å data that can be linked directly with CMEs observed with the LASCO coronagraph. Examples include the halo CME associated with the EIT wave of May 12, 1997 (Thompson et al. 1998; Plunkett et al. 1998) and the CMEs of January 25 1998 (Gopalswamy et al. 1998) and 23 December 1996 (Dere et al. 1997). Delannée et al. (2000) examine EIT 195 Å data for a period of 6 days between 1 and 6 November 1997 and find that of 17 ejections observed in this data, 13 are related to white light CMEs in LASCO data.

Several studies have been carried out on associating CMEs with other kinds of solar activity such as flares and disappearing prominences. Munro et al. (1979) used CME observations from Skylab data during 1973-1974 near solar minimum in conjunction with reports of associated activity from the Solar Geophysical Data archives. They found that 78% of the CMEs observed were associated with other forms of solar activity. Of these, they found that 40% of the CMEs observed are associated with flares, while more than 70% of CMEs are associated with eruptive prominences (with and without flares). Webb & Hundhausen (1987) examined SMM data during 1980 near solar maximum and found that 66 % of the CMEs observed were associated with other forms of solar activity. Of these, they found that 68% of the observed CMEs were associated with erupting prominences, 37% with H $\alpha$  flares and 47% with X-ray events. St. Cyr & Webb (1991) analyzed SMM data from 1984–1986, during the declining phase of the solar cycle. They find that slightly less than half of the CMEs have associations with other forms of solar activity. Of these, they found that 76% were associated with erupting prominences, 26% with H $\alpha$  flares and 74% with X-ray events. Gilbert et al. (2000) have analyzed H $\alpha$  data from the Mauna Loa Solar Observatory and LASCO data to study the relationship between prominence activity and CMEs. Their data cover the period February 1996 – June 1998, which is very similar to the period covered in our study. One of their principal findings is that 94% of eruptive prominences discerned in the H $\alpha$  data had CMEs associated with them.

We now review recent work examining the relation between CMEs and the photospheric magnetic field. Feynman & Martin (1995) find a strong correlation between newly emerging magnetic field and filament eruptions, which they take to be proxies for CMEs. Luhmann et al. (1998) employ potential field extrapolations to determine the large scale coronal field from the photospheric magnetic field. Their results suggest that although the changes in the small scale photospheric magnetic field before and after a CME might be indiscernible, CMEs could correspond to the opening up of large scale coronal field lines.

Lara, Gopalswamy & DeForest (2000) examine 8 eruptive events associated with active regions during 1997 and 1998. They find that the total magnetic flux over an active region did not show significant changes. However, they found significant changes in the flux over small subregions of the overall active region associated with the CMEs. They also found that the changes in flux occur over timescales of several hours to days.

Photospheric magnetic field configurations are the boundary conditions for determining the coronal magnetic field which is disrupted during a CME. Canfield, Hudson & McKenzie (1999) have suggested that CME source regions often correspond to structures resembling sigmoids in YOHKOH soft X-ray images, that presumably trace highly stressed coronal magnetic field configurations.

The issue of CME initiation is thus an issue of considerable contemporary interest. The combination of the highly sensitive white light images provided by the LASCO coronagraph, on-disk EIT images and 1.5 hour cadence (MDI) photospheric magnetograms provide a unique opportunity to investigate the complex question of CME initiation. This kind of comprehensive data set was not available when previous studies, described above, of the associations between CMEs and disk phenomena were made. We address the question of CME initiation by analyzing the source regions of CMEs observed on the solar disk in EIT 195 Å images during the solar minimum period of January 1996–June 1998.

## 2. Data Analysis Procedure

Our main aim in this paper is to determine the source regions of CMEs as seen in EIT 195 Å images, understand the signatures of CMEs in the low corona and compare them with underlying photospheric magnetic field configurations. Line-of-sight magnetograms measure the longitudinal component of the magnetic field. The magnetograms we use

from the NSO Kitt Peak and the MDI instrument are most sensitive near disk center, since there is no foreshortening. Accordingly, we have searched the LASCO CME database (<http://lasco-www.nrl.navy.mil/cmelist.html>) for the period January 1996 - June 1998 to find CMEs in white light LASCO images that have clear on-disk transients in EIT 195 Å images associated with them. We search EIT 195 Å images within approximately 20-25 minutes prior to the appearance of the CME in the LASCO C2 field of view to see if there are identifiable transients that could correspond to the initiation of the CME in the lower corona. Such signatures include plasma/material motions, transient coronal holes/dimming (Sterling & Hudson 1997; Zarro et al. 1999), erupting prominences and EIT waves (Thompson et al. 1999) and flares. We have generally restricted ourselves to CMEs

- that have unambiguous associations with on-disk phenomena observed in EIT 195 Å images, and
- where there are high cadence (12-18m), full resolution (2.6 arc-sec/pixel) EIT 195 Å images so that the initiation and source region of the CME-related transients in 195 Å EIT images is clearly evident.

We have cataloged a total of 32 events that satisfy the above-mentioned criteria during the solar minimum period of January 1996–June 1998 (Table 1). Since this is only a fraction of the CMEs observed by LASCO during this time period, it is necessary to consider the effect that our selection criteria might have on our final conclusions. First, the selected CMEs only refer to a specific time period near the rising phase of solar cycle 22 and may not be tightly correlated with other phases of the solar cycle. However, the correlation of CMEs observed with SMM with other forms of solar activity at solar maximum (Webb & Hundhausen 1987) and during the declining phase (St. Cyr & Webb 1991) were similar and suggest that the correlations found in the present study may be more generally applicable to

other phases of the solar cycle. Our conclusions will certainly be affected by the relatively small number of events in our selection but we expect the basic conclusions to be broadly representative of this phase of the solar cycle. The criteria used to select the events we have examined were arrived at for the purpose of a clear determination of the source region and the short term photospheric magnetic field activity related to the CME. The signatures of CMEs in the EIT data are often subtle so that the availability of high cadence EIT data is necessary for a clear location of the source region. Since there were few high cadence EIT 195 Å observations before March 1997 because of telemetry restrictions, our data is biased towards events from March 1997 onwards. The MDI photospheric magnetograms are the only consistent set of data available for studying photospheric field evolution at a reasonable cadence. Since the magnetic sensitivity of MDI drops off toward the limb, these data are best used near disk center. Consequently, we believe that the conclusions of this study have been strengthened by limiting our list of CMEs to a well-observed subset of all of the CMEs observed by LASCO during our period of study.

### **3. Results**

#### **3.1. Aggregate Results**

We have recorded the heliographic coordinates of the source region of the CME related transient in 195 Å EIT images for each event. We have superimposed the heliographic positions of these source regions on synoptic magnetograms available from NSO Kitt Peak. If the outline of the CME source region lies over an active region, we conclude that it is active region related. During this phase of the solar cycle, active regions are usually well isolated and these identifications tend to be straightforward. Two examples of synoptic magnetograms with CME source regions superimposed are shown in Figures 1a and 1b. We have carried out this procedure for all the 32 events in our catalog (Table 1), but we do not

show all the relevant synoptic magnetograms for lack of space.

We have employed a variety of sources to ascertain whether a CME is associated with an erupting prominence.  $H\alpha$  data from the Big Bear Solar Observatory (BBSO) and the Observatory of Paris at Meudon and some other sources like the Holloman Air Force Base and the Hiraïso Solar Terrestrial Research Center often help to show whether a prominence existed near the source region of the CME related transient. Prominence eruptions are occasionally clearly evident in EIT 195 Å data as cool prominence material seen in absorption or as bright ejecta seen in emission. We have also examined EIT 304 Å data for prominences, but this is usually not very useful because the time interval between images is typically as large as 6 hours. Erupting prominences are also occasionally clearly evident in LASCO C2 data as highly structured material. We have also used Solar Geophysical Data reports of prominence eruptions.

This exercise allows us to place the source regions of CMEs into the following broad categories (see Table 1):

1. CME source regions that are co-spatial with active regions (AR category).

Prominences are sometimes embedded in these active regions, but there is no evidence to suggest that any part of it erupted with the CME.

2. CME source regions that are related to eruptions of prominences that were embedded in active regions (AR+EP category). In some cases, the entire embedded prominence erupts as part of the CME, while in others only part of the prominence does so.

The prominences in this category are often embedded in old, decaying active regions. Such regions might not necessarily be assigned a NOAA active region number. We have labelled some events in this category as AR+(EP). These are events for which evidence for eruption of a prominence embedded in the active region is not very conclusive.



3. CME source regions that are related to eruptions of prominences outside active regions (EP category). The prominences in this category occur in quiet regions where the magnetic fields are relatively weak.

The association of CME source regions with active regions (events in category 1) is made by visual inspection of EIT 195 Å images and synoptic magnetograms. The association with erupting prominences, on the other hand, is made by inspecting data from various sources as described above. Table 1 gives a short summary of all the events considered in this study. As summarized in Figure 2, we find that 13 (41%) of the cataloged events fall in the AR category, while 14 (44%) are in the AR+EP category and 5 (15%) are in the EP category. We have included events labelled as AR+(EP) in Table 1 in the count for AR+EP events.

Feynman & Martin (1995) find that quiescent filament eruptions (which they take to be proxies for CMEs) are strongly correlated with emergence of new magnetic flux over several days preceding the eruption. Our findings in this respect are different. As shown in Figure 2, 14 of the 32 events on our list are in the AR+EP category, which was not included in the study by Feynman & Martin (1995), while 5 of the 32 events on our list are in the EP category. The CMEs in the EP category arise from eruptions of prominences outside active regions. There is no evidence for significant large-scale emerging magnetic flux for any of the 5 events in the EP category. Nevertheless, we have observed quiescent filament eruptions that were associated with newly emerged magnetic flux, for example, the west limb CME on 1996 July 10. This event was not included in our study because of the lack of high cadence EIT data.

Of the 14 events in the AR+EP category, we find that 4 are associated with emerging magnetic flux. For 3 of these 4 AR+EP events, the flux emerges over timescales of  $\sim 7$ –27 days. Only 1 of these 4 events shows flux emergence over a timescale of  $\sim 1$  day. Our

conclusions regarding emergence or cancellation of magnetic flux (or the lack thereof) are based on detailed visual inspection of MDI magnetograms before and after the event.

### 3.2. Case Studies

Sorting the various CMEs into 3 categories provides a useful overall description of the source regions of CMEs. Nevertheless, such a broad characterization covers over much of the complexity of the nature of the CME source regions and the CME initiation. We have therefore selected 6 especially well observed events from the list of 32 events for closer examination (Table 2). The principal criterion used in the selection of this subset of 6 events was the availability of high cadence EIT 195 Å images. For these events, we have examined the EIT 195 Å images in detail and made detailed visual comparisons of the EIT 195 Å images with full disk photospheric magnetograms from the MDI instrument in order to determine the spatial and temporal relationship between the photospheric magnetic field evolution and the CME-related transient in EIT 195 Å images. We have also examined X-ray light curves from GOES data to determine if there are flares associated with each of these events. In particular, we have referred to the X-ray flare classification based on GOES X-ray data in the 0.1-0.8 nm band that is used in the Solar and Geophysical Data reports.

#### 3.2.1. *The CME of 01 April 1997*

This is an example of an active region (AR) associated CME and is associated with active region 8026 (lower panel of Figure 3a) during Carrington rotation 1921. The active region was absent on the previous rotation, and emerged on the back side of the sun after 14 March 1997. Since it is an isolated active region, loops associated with this AR can be discerned from LASCO C1 images as early as 22 March 1997, well before the AR reaches

the East limb. The AR rotates into view in NSO Kitt Peak magnetograms close to the East limb during rotation 1921 on 27 March 1997 (S23E78). The CME of 01 April 1997 occurs when the AR is at S24E20 (Figure 3a). Following the CME, the active region weakens and disperses, but retains its identity well into rotation 1922. It was last seen near the west limb on 13 May 1997 during rotation 1922 in MDI magnetogram data and does not reappear at the east limb on 26 May 1997. In summary, the active region, with which the CME of April 1 1997 is associated, appeared between 14 March 1997 and 22 March 1997 and disappeared between 13 May 1997 and 26 May 1997. The lifetime of the active region is between 53 and 75 days. The CME occurred early in the life of the active region.

AR 8026 consists of two compact regions of opposite magnetic polarities, with a parasitic negative polarity embedded in the positive polarity region (Figure 3a). On 01 April 1997, the sunspot corresponding to AR 8026 is assigned a  $\beta$  classification. The parasitic negative polarity region is evident in the MDI magnetogram images from as early as 23:59 UT on 1997/03/31. Upon comparing the two upper panels of Figure 3a, it is evident that the parasitic negative polarity evolves from being embedded in the positive polarity region at 08:03 UT to forming a lane between two segments of the positive polarity region by 14:27 UT. This trend continues, and we find that the negative parasitic polarity lane has elongated further by 17:39 UT. On 1 April 1997, the MDI magnetograms show a fair amount of small-scale flux emergence and cancellation, particularly along the neutral line and the western edge of the active region.

Near the time of the CME, the first sign of activity in EIT 195 Å images is a brightening at 13:25 UT apparently at the top of the arch connecting the dominant polarities of AR 8026 (upper panel of Figure 3b). This is followed by a brightening at 13:46 UT near the eastern leg of the bipolar arch, around the location of the parasitic polarity (lower panel of Figure 3b). The brightening near the parasitic polarity is clearly evident in the straight

EIT 195 Å image at 14:00 UT (Figure 3c). This sequence of events is accompanied by an M1.9 X-ray flare that starts at 13:25 UT, peaks at 13:48 UT and ends at 14:01 UT. An EIT wave is observed to emanate from the vicinity of the active region at 14:00 UT (lower panel of Figure 3b). The northwestern front of this disturbance is the only one that can be clearly identified as an outwardly propagating feature in successive images. It starts out with a velocity of  $\sim 100 \text{ km s}^{-1}$  and propagates with an acceleration of  $\sim 70 \text{ ms}^{-2}$ . By the time it reaches the northwest edge of the disk, it has attained a speed of  $\sim 300 \text{ km s}^{-1}$ . A stationary dimming region is observed to the southwest of the active region. It is manifested as a deepened darkening at approximately the same location in the running difference EIT 195 Å image at 14:18 UT. We also observe a stationary transient dimming at 14:18 UT to the southeast of the active region. We have checked constant base difference EIT 195 Å images to verify that these features are not artifacts of the running difference technique. In summary, the activity observed in EIT 195 Å images consists of a flare(s), an EIT wave propagating towards the northwest and dimming regions to the southeast and southwest of the active region.

The LASCO C2 observations of the CME are shown in Figure 3d. These running difference LASCO C2 images show a wide, bright mound on the east limb appearing simultaneously with a small bright ejection on the west limb at 15:18 UT. The wide front on the east limb travels outward at a speed of  $296 \text{ km s}^{-1}$  (<http://lasco-www.nrl.navy.mil/cmelist.html>). The appearance of this CME is considerably different from those that are typically ejected from the limb but is consistent with a CME ejected from the solar disk in the general direction of SOHO. The simultaneous ejection from the two limbs suggests that this CME could be a toroidal CME (Brueckner et al. 1998) propagating towards the earth. It is worth noting that the EIT wave propagates to the northwest, whereas the CME observed in LASCO C2 images is concentrated along the equator, with the brightest feature on the east limb. Consequently, the propagating front in EIT 195 Å

data is probably not directly related to the white light CME. However, the visibility of the EIT wave on the disk could be non-uniform, and the northwestern feature could be the most evident one. Furthermore, CMEs originating near the limb that start out propagating at relatively large angles to the equator eventually tend to follow the large-scale dipole field and bend towards the equator as they propagate out.

### *3.2.2. The CME of 21 October 1997*

This event is classified in the AR+EP category. The source region of this CME is the old, decaying active region complex that includes AR 8097 and the magnetic fields to its northeast (Figure 4a). Synoptic magnetograms from the NSO Kitt Peak reveal that this active region complex emerges during Carrington rotation 1926. It then undergoes considerable evolution, but does not disappear until Carrington rotation 1932. The lifetime of the overall complex is thus  $\sim 6$  months, and this CME occurs  $\sim 3$  months after the complex first appeared. The emergence of AR 8097 represents the emergence of new flux into the original active region complex. AR 8097 was not present at the west limb during rotation 1927 on 02 October 1997. It grew on the backside of the Sun and rotated into view at the East limb in Kitt Peak NSO magnetogram data on 16 October 1997 (Carrington rotation 1928). There was evidence for loops associated with this active region in EIT 195 Å images when this active region was behind the east limb, on 14 October 1997. We therefore conclude that AR 8097 emerged between 02 October 1997 and 14 October 1997. Synoptic magnetograms from the NSO Kitt Peak reveal that this active region decayed slowly and disappeared between 13 January 1998 and 12 February 1998. There is evidence for small-scale flux emergence, cancellation and decay in the photospheric magnetic field (Figure 4a), but the relation of these changes to the activity in EIT 195 Å images is not clear. In summary, the CME of 21 October 1997 occurred during the rising phase of new

flux injected into an old, decaying active region complex.

The activity observed in the EIT 195 Å images includes a bright EIT wave accompanied by propagating density depletions, a possible prominence ejection, ejection of bright material to the southeast and flare-associated brightenings. The EIT 195 Å images available around the time of this event suggest that an EIT wave is initiated from AR 8097 between 16:18 UT and 17:34 UT. The top panel of Figure 4b shows the pre-initiation state of the EIT wave at 16:18 UT, while the bottom panel shows the EIT wave in progress at 17:45 UT. Unfortunately, there is no EIT 195 Å data between 16:18 and 17:34. The wave is observed to spread in a semi-isotropic manner, propagating preferentially towards the south. The most pronounced wave-associated darkenings (which could be interpreted as density depletions) are observed towards the north and south of the active region. The propagating depletion wave is also accompanied by material ejection that is manifested as the bright N–S feature at the southwestern boundary of the dark region in the lower panel of Figure 4b. This event is accompanied by a C3.3 flare that starts at 17:00 UT, peaks at 17:54 UT and ends at 18:16 UT. At 17:34 UT we observe a bright linear feature near the magnetic neutral line that we interpret as the prominence activation. Later, at 17:45 UT, we observe a double-ribbon flare-associated brightening on either side of the prominence and at the footpoints of the post-flare loops which are later seen in EIT 195 Å images at 18:12 UT (Figure 4c).

There is some evidence for an erupting prominence from EIT 195 Å images; a dark feature embedded in the active region is seen to travel outward after 16:18 UT. Also, at 17:34 a bright linear feature is seen along the neutral line between the two flare ribbons that are seen later in the flare. Furthermore, an H $\alpha$  6563 Å image from the Big Bear Solar Observatory taken at 15:26 UT on 21 October 1997 reveals an embedded filament in the active region. The corresponding image taken at 15:45 UT on 22 October 1997 shows that the embedded filament has largely disappeared. It is therefore quite likely that this CME

is associated with the eruption of a part of this embedded prominence. Consequently, we have placed this CME in the active region with prominence (AR+P) category.

This sequence of events is associated with a halo CME at 18:18 UT in LASCO C2 data (Figure 4d). The CME front is brightest on the east limb, although a faint front extends all over the northern hemisphere. The southwestern front of the halo is somewhat delayed with respect to the other fronts. The leading edge on the east limb travels outward at a speed of  $465 \text{ km s}^{-1}$ , with no appreciable acceleration.

### *3.2.3. The CME of 20 January 1998*

The source of this CME is placed in the AR category. The source region of this CME is the compact active region 8135 (lower panel of Figure 5a). On 20 January 1998, AR 8135 is associated with a  $\beta$  sunspot. There was no evidence for this active region at the west limb on 01 January 1998 during rotation 1930. AR 8135 appears near the East limb in Kitt Peak magnetogram data on 13 January 1998. EIT 195 Å images show evidence for this active region until as far as 24 January 1998. Since this is a fairly weak active region, it is difficult to discern if it survives beyond 24 January 1998, either from EIT 195 Å or from MDI magnetogram data. It is, however, clear that this active region does not appear at the East limb during rotation 1931 on February 6 1998. We therefore conclude that AR 8135 appeared between 01 and 13 January 1998 and disappeared between 24 January 1998 and 6 February 1998. The lifetime of AR 8135 is fairly short, between 11 and 36 days. The CME of 20 January 1998 occurred roughly midway during the lifetime of the active region.

A comparison of the top left and top right panels of Figure 5a reveals flux cancellation to the south of the dominant polarities in the active region over a 6 hour timescale. There was no evidence for an erupting prominence in this active region. This event is therefore an

example of those in the active region (AR) category.

The EIT 195 Å images of Figure 5b show the development of a transient dumbbell shaped depletion region behind faint loop-like structures. The depletion region starts forming at 20:53 UT and deepens by 21:05 UT and extends to the north and south of AR 8135. Constant base difference images also show this depletion region. The faint loop-like structures appear to connect opposite magnetic polarity with high field strength as seen in the MDI images. Unlike some of the events previously described, the outward propagation of the depletion region is very limited. This suggests that the dimming is not an EIT wave.

The activity seen in EIT 195 Å images is associated with the a faint CME on the west limb. The first signs of this CME in LASCO C2 images are observed at 22:03 UT. Figure 5c shows the successive stages of the CME as it develops and propagates outward. The leading edge of the CME travels outward at a speed of  $253 \text{ km s}^{-1}$  with no appreciable acceleration (<http://lasco-www.nrl.navy.mil/cmelist.html>). As with the AR event of 01 April 1997, the direction of motions observed in EIT 195 Å images do not appear to be well correlated with the CME seen in LASCO C2 images; while the density depletion formed in the southwest, the CME was observed over the west limb. However, as mentioned before, it is possible that the large scale dipole field channeled the CME that originated in the lower corona towards the equator. There is no evidence of a flare associated with this event. A C1.5 flare occurred between 19:32 UT and 19:46 UT, but it was evidently not associated with the sequence of events related to this CME.

#### *3.2.4. The CME of 25 January 1998*

This is a fairly complex event that has been classified in the AR+EP category. This CME has also been studied in some detail by (Gopalswamy et al. 1998). It involves a newly



emerged active region AR 8145 and decaying active region flux that contains a quiescent filament. The decaying active region complex shown in Figure 6a has a lifetime of  $\sim 7$  months, first appearing during Carrington rotation 1927 and disappearing by rotation 1933.

During the previous rotation (1931), there was no evidence for AR 8145 near the west limb on 11 January 1998. AR 8145 grew on the backside of the sun and came into view during rotation 1932 near the east limb in MDI magnetogram data on 24 January 1998. MDI magnetogram data shows that AR 8145 retains its identity until it is close to the west limb on 03 February 1998 during rotation 1932, but does not appear on the east limb on 16 February 1998 during the subsequent rotation. AR 8145 appeared between 11 January and 24 January 1998 and disappeared between 03 February and 16 February 1998. Its lifetime is thus between 11 and 37 days. Either way, it is evident that the CME of 25 January 1998 occurred during the rising phase of the active region. Since AR 8145 is fairly close to the limb around the time of the CME, projection effects limit our ability to discern short-term changes in the photospheric magnetic field.

This CME occurs  $\sim 6$  months after the overall complex first appeared, during rotation 1932. Unlike the AR+EP CME of 21 October 1997, this CME does not seem to be associated with emerging flux into the old, decaying active region complex. However, the EIT 195 Å images of Figure 6c, which show the latter stages of development of the CME suggest that the large-scale fields associated with this CME are rooted in AR 8145 towards the east of the decaying active region complex.

The EIT 195 Å images of Figure 6b show an EIT wave and an erupting prominence starting at 14:19 UT. Figure 6c shows the latter stages of evolution of the erupting filament and the associated EIT wave. The EIT wave is comprised of a depletion region behind a bright front. As before, we have examined constant base difference images to verify that the depletion and brightenings are not merely artifacts of the running difference technique.

At around 14:32 UT, the depletion region develops and propagates to the southeast. By 15:02 UT, the bright front of the EIT wave have covered a substantial portion of the solar disk. This sequence of events is accompanied by a C1.1 X-ray flare that starts at 14:29 UT, peaks 15:12 UT and ends at 17:00 UT. The post-flare loop brightenings evident in Figure 6c are primarily concentrated across the neutral line of the old active region fields.

The EIT He II 304Å image at 13:47, one of 4 synoptic 304Å images obtained on that day, shows a filament that gives the impression of lifting off from the old active region neutral line. The time series of EIT 195Å images indicates that the hot ejecta that also participate in the CME observed in LASCO C2 originate in the newly emerged AR 8145 at 14:19. Other ejecta also appear from the south-west of the old active region flux. It is possible that Feynman and Martin would have classified this event as a quiescent filament eruption that was associated with the emergence of new, nearby magnetic flux. The orientation of the polarities of the new flux is likely to result in a reconnection of magnetic flux between the new and the old flux system.

A very bright CME is observed above the east edge of the LASCO C2 occulter at 15:26 (Figure 6d). This CME is a partial halo but the halo signatures are most prominent to the south.

### *3.2.5. The CME of 03 May 1998*

The source region of the 1998 May 3 CME is of the AR+EP type. The source region AR 8210 is the prolific source of several CMEs between 27 April 1998 and 06 May 1998 during rotation 1935. It was absent at the west limb on 16 March 1998, during rotation 1933. It grew on the backside of the sun and rotated into view at the east limb on 29 March 1998 during rotation 1934. AR 8210 rotates into view at the east limb on 25 April 1998

during rotation 1935. AR 8210 is close to the west limb on 08 May 1998 during rotation 1935. A considerably weakened version of this active region rotates into view on the east limb during rotation 1936 on 21 May 1998. It disappears during its passage across the disk between June 2 and June 3 1998. In summary, the active region appeared between 16 March and 29 March 1998 and disappeared around 3 June 1998. The overall active region lifetime is thus  $\sim 65$ -79 days. This is a prolific active region that produced several CMEs and large flares during its transit across the disk during rotation 1935 (Table 3). All the CMEs that originate from this active region between 27 April 1998 and 06 May 1998 (Table 3) take place roughly during the mid-phase of this active region. Figure 7a shows MDI magnetogram images of AR 8210 around the time of the CME. The lower panel of Figure 7a shows the position of AR 8210 on the solar disk, while the upper panels show closeups of the active region. On 03 May 1998, AR 8210 is associated with a  $\beta$ - $\gamma$ - $\delta$  sunspot. It can be seen that there is small scale flux cancellation in the areas marked by the black arrows over a timescale of  $\sim 6$  hours prior to the initiation of the CME of 03 May 1998. The general level of small-scale flux emergence and cancellation in this active region is considerably enhanced over other source regions discussed in this paper. The strength of this activity may be related to high rate of CME production.

On May 03 1998, the first sign of activity in EIT 195 Å data is a brightening in the central part of AR 8210 at 21:25 UT. Bright prominence material is also ejected to the north in EIT 195 Å data at 21:25 UT. This is followed by propagation of a density depletion towards the north accompanied by material ejection at 21:39 UT (upper panel of Figure 7b). The brightening of AR 8210 continues, and the patchy transient density depletion covers most of western half of disk by 21:57 UT (lower panel of Figure 7b). This sequence of events is accompanied by an M1.4 flare that starts at 21:12 UT, peaks at 21:29 UT and ends at 21:49 UT. The CME is first observed in the LASCO field of view over the northwest limb at 22:02 UT (Figure 7c), propagating outwards with an initial speed of  $639 \text{ km s}^{-1}$

(<http://lasco-www.nrl.navy.mil/cmelist.html>). In the C2 field of view, the CME propagates to the northwest even though its active region source lay in the southern hemisphere.

### 3.2.6. *The CME of 19 May 1998*

This is an example of a CME that falls in the EP category (Figure 2). The prominence is formed along the neutral line of the relatively weak, extended magnetic fields to the west of AR 8222 (Figure 8a). These fields appear to be the dispersed remnants of AR 8203 which emerged during the previous rotation (rotation 1935). We studied the active region and the weaker magnetic fields to its west for a period of 5 days before the CME. We found no evidence for significant large-scale emerging or cancelling flux near the location of the prominence over this timescale. A comparison of the upper and lower panels of Figure 8a shows that there are no significant small-scale changes in magnetic flux over timescales of a few hours either.

The EIT 195 Å images of Figure 8b and 8c show the prominence eruption starting at 09:34 UT. The entire prominence disappears in unison. The eruption is well in progress by 09:56 UT. In particular, the erupting prominence is clearly evident in the straight EIT 195 Å image of Figure 8b. The prominence eruption results in the CME in LASCO C2 data shown in Figure 8d. The prominence is clearly evident as the bright filamentary structure in the right panel of Figure 8d. There was a C4 flare associated with this CME.

## 4. Discussion and Conclusions

We have surveyed 32 CMEs during January 1996 - June 1998 whose source regions are well observed on the solar disk in EIT 195 Å images. All these CMEs occurred near solar minimum during the rising phase of cycle 21, and are tabulated in Table 1. As depicted in

Figure 2, we find that 13 (41%) of these events are associated with active regions without prominence eruptions, 14 (44%) are associated with eruptions of active region prominences, and 5 (15%) are associated with eruptions of prominences outside active regions. Of the 14 CMEs that are associated with eruptions of active region prominences, 4 show evidence for emerging magnetic flux over several days before the CME.

These statistics contrast with those obtained from Skylab and SMM observations (Munro et al. 1979; Webb & Hundhausen 1987; St. Cyr & Webb 1991) which find that a significantly larger fraction of CMEs are associated with prominence eruptions. However, the differences between these studies should be kept in mind: the current study considers only those CMEs that have on-disk counterparts in EIT 195 Å data. On-disk CMEs are considered because we wish to compare the CME source regions with the underlying photospheric magnetic field, and longitudinal magnetograms are more reliable when observed close to disk center. The studies made with Skylab and SMM data, (Munro et al. 1979; Webb & Hundhausen 1987; St. Cyr & Webb 1991) on the other hand, mostly consider CMEs seen on the limb. None of these studies had accompanying full-disk EUV data. The association of CMEs with prominences in these studies was made by considering prominences within specified latitudinal and longitudinal ranges of the CME locations as inferred from white light coronagraph data.

We have described 6 especially well observed events from our overall catalog of 32 CMEs that have identifiable on-disk signatures in EIT 195 Å images. The principal criterion used in selecting these 6 events was the availability of high resolution, high cadence EIT 195 Å data. We have discussed these events in some detail in §3.2. We have abstracted some salient characteristics from these descriptions in Table 2. It suggests that active region CMEs (AR) are associated with active regions with lifetimes ranging from  $\sim$  11-80 days. These CMEs occur either during the rising phase or mid-life of the active regions.

AR CMEs are also often associated with growing parasitic polarity magnetic fields or with cancelling magnetic flux over timescales of  $\sim 6$  hours near the initiation time of the CME. It should be emphasized that such changes in magnetic flux take place over timescales that are much longer than the timescale over which the CMEs are initiated. While these changes in the photospheric magnetic field take place over timescales of around 6-7 hours, the CME initiation processes typically take place over timescales of  $\sim 30$  minutes - 1 hour. Furthermore, there is no particularly distinguishing feature that sets these changes in the photospheric magnetic field apart from similar changes in other non-CME producing active regions, based on a fairly non-critical study. CMEs that result from erupting active region prominences (AR+EP), are associated with old, decaying active regions with lifetimes greater than 6 months.

PS acknowledges several useful discussions with Dr. Angelos Vourlidas. We acknowledge several useful comments and suggestions from the anonymous referee.

This work was made possible with funding from NASA. SOHO is a project of international cooperation between ESA and NASA. The SOHO/LASCO data used in this paper are produced by a consortium of the Naval Research Laboratory, Max-Planck-Institut fuer Aeronomie (Germany), Laboratoire d'Astronomie (France), and the University of Birmingham (England). We gratefully acknowledge the SOHO SOI/MDI team for use of data from the MDI instrument. We thank the Big Bear Solar Observatory and the Observatory of Paris at Meudon for making their data available on the SOHO synoptic data webpage. NSO/Kitt Peak data used here are produced cooperatively by NSF/NOAO, NASA/GSFC, and NOAA/SEL.

## REFERENCES

- Brueckner, G. E., Delaboudinière, J.-P., Howard, R. A., Paswaters, S. E., St. Cyr, O. C., Schwenn, R., Lamy, P., Simnett, G. M., Thompson, B. J., and Wang, D., 1998, *Geophys. Res. Lett.*, 25, 3019
- Canfield, R. C., Hudson, H. S., McKenzie, D. E., 1999, *Geophys. Res. Lett.*, 26, 627
- Delannée, C., Delaboudinière, J.-P., and Lamy, P. 2000, *A&A*, 355, 725
- Dere, K. P., et al. 1997, *Sol. Phys.*, 175, 601
- Dere, K. P., et al. 2000, *Sol. Phys.*, 195, 13
- Feynman, J., and Martin, S. F., 1995, *J. Geophys. Res.*, 100, 3355
- Gilbert, H. R., Holzer, T. E., Burkepile, J. T., and Hundhausen, A. J. 2000, *ApJ*, 537, 503
- Gopalswamy, N., Yashiro, S., Kaiser, M. L., Thompson, B. J. and Plunkett, S. P. 1998, in *Solar Physics with Radio Observations, Proceedings of Nobeyama Symposium*, eds. T. Bastian, N. Gopalswamy and K. Shibasaki
- Lara, A., Gopalswamy, N., and DeForest, C., 2000, *Geophys. Res. Lett.*, 27, 1435
- Luhmann, J. G., Gosling, J. T., Hoeksema, J. T., and Zhao, X., 1998, *J. Geophys. Res.*, 103, 6585
- Munro, R. H., Gosling, J. T., Hildner, E., MacQueen, R. M., Poland, A. I., and Ross, C. L., 1979, *Sol. Phys.*, 61, 201
- Plunkett, S. P., Thompson, B. J., Howard, R. A., Michels, D. J., St. Cyr, O. C., Tappin, S. J., Schwenn, R. and Lamy, P. L. 1998, *Geophys. Res. Lett.*, 25, 2477
- Sterling, A. C., and Hudson, H. S., 1997, *ApJ*, 491, L55

St. Cyr, O. C., and Webb, D. F., 1991, *Sol. Phys.*, 136, 379

Thompson, B. J., Plunkett, S. P., Gurman, J. B., Newmark, J. S., St. Cyr, O. C., Michels, D. J. and Delaboudinière, J.-P. 1998, *Geophys. Res. Lett.*, 25, 2461

Thompson, B. J., Gurman, J. B., Neupert, W. M., Newmark, J. S., Delaboudinière, J.-P., St. Cyr, O. C., Stezelberger, S., Dere, K. P., Howard, R. A., and Michels. D. J., 1999, *ApJ*, 517, L151

Webb, D. F., and Hundhausen, A. J., 1987, *Sol. Phys.*, 108, 383

Zarro, D. M., Sterling, A. C., Thompson, B. J., Hudson, H. S., Nitta, N., 1999, *ApJ*, 520, L139



Fig. 1a.— The background is the synoptic magnetogram from the Kitt Peak NSO for Carrington rotation 1931. The on-disk CMEs observed in EIT 195 Å data during this rotation are superimposed on the magnetogram.

Fig. 1b.— The background is the synoptic magnetogram from the Kitt Peak NSO for Carrington rotation 1932. The on-disk CMEs observed in EIT 195 Å data during this rotation are superimposed on the magnetogram. We have examined such magnetograms for rotations 1915-1935. We show only two examples here in order to conserve space.

Fig. 2.— This figure gives the number of on-disk CMEs in each of the categories AR, AR+EP and EP. Of the 32 on-disk CMEs recorded in EIT 195 Å data, 13 are associated with active regions (AR), 5 with eruptions of prominences outside active regions (EP) and 14 with eruptions of active region prominences (AR+EP).

Fig. 3a.— MDI magnetogram data for AR 8026, which was the source region for the CME of 01 April 1997. The bottom panel shows the location of the overall active region on the solar disk, while the top panels show a closeup of the active region. The parasitic negative polarity (marked by the black arrow on the top panels) grows over a timescale of  $\sim 6$  hours near the CME initiation time to form a lane in the midst of the positive polarity region. The CME starts developing on the disk as seen in EIT 195 Å images around 13:46 UT, and the parasitic polarity continues to grow and form the lane well beyond 14:27 UT.

Fig. 3b.— Running difference EIT 195 Å images that show the development of the CME of 01 April 1997. Contours of the photospheric magnetic field from MDI data are superimposed. The red contours denote +10 gauss fields, yellow +50 gauss, blue -10 gauss and green -50 gauss.

Fig. 3c.— Straight EIT 195 Å image showing part of the flare associated with the CME of 01 April 1997. Contours of the photospheric magnetic field from MDI data are superimposed. The red contours denote +10 gauss fields, blue -10 gauss, yellow +50 gauss and green -50 gauss. It can be seen that the flare occurs at the location of the parasitic negative polarity.

Fig. 3d.— Running difference images from the LASCO C2 coronagraph showing the development of the CME of 01 April 1997. The inner white circle in the center is at  $1 R_{\odot}$  while the outer circle is the boundary of the C2 occulter at  $2.2 R_{\odot}$ .

Fig. 4a.— MDI magnetogram data showing AR 8907 and the associated decaying active region complex to its northeast. The CME of 21 October 1997 was associated with the eruption of a filament above the neutral line of the decaying active region complex.

Fig. 4b.— Running difference EIT 195 Å images that show the development of the CME of 21 Oct 1997. Contours of the photospheric magnetic field from MDI data are superimposed. The red contours denote +10 gauss fields, blue -10 gauss, yellow +50 gauss and green -50 gauss.

Fig. 4c.— Straight EIT 195 Å images showing the flaring activity associated with the CME of 21 Oct 1997. The twin ribbon configuration evident in the lower panel is of special interest. Contours of the photospheric magnetic field from MDI data are superimposed. The yellow contours denote +50 gauss fields and the green contours -50 gauss fields.

Fig. 4d.— Running difference images from the LASCO C2 coronagraph showing the development of the CME of 21 Oct 1997. The inner white circle in the center is at  $1 R_{\odot}$  while the outer circle is the boundary of the C2 occulter at  $2.2 R_{\odot}$ .

Fig. 5a.— MDI magnetogram data for AR 8135, which was the source region for the CME of 20 Jan 1998. The bottom panel shows the location of the overall active region on the solar disk, while the top panels show a closeup of the active region. The top panels show flux cancellation near the area marked by the white arrows over a  $\sim 6$  hour timescale before the initiation of the CME in EIT 195 Å data.

Fig. 5b.— Running difference EIT 195 Å images that show the development of the CME of 20 Jan 1998. Contours of the photospheric magnetic field from MDI data are superimposed. The red contours denote +10 gauss fields, blue -10 gauss, yellow +50 gauss and green -50 gauss.

Fig. 5c.— Running difference images from the LASCO C2 coronagraph showing the development of the CME of 20 Jan 1998. The inner white circle in the center is at  $1 R_{\odot}$  while the outer circle is the boundary of the C2 occulter at  $2.2 R_{\odot}$ .

Fig. 6a.— MDI magnetogram data showing AR 8145 and the associated decaying active region complex to its west. The CME of 25 Jan 1998 was associated with the eruption of a filament above the neutral line of the decaying active region complex.

Fig. 6b.— Running difference EIT 195 Å images that show the development of the CME of 25 Jan 1998. Contours of the photospheric magnetic field from MDI data are superimposed. The red contours denote +10 gauss fields, blue -10 gauss, yellow +50 gauss and green -50 gauss.

Fig. 6c.— Running difference EIT 195 Å images that show the latter stages of development of the CME of 25 Jan 1998.

Fig. 6d.— Running difference images from the LASCO C2 coronagraph showing the development of the CME of 25 Jan 1998. The inner white circle in the center is at  $1 R_{\odot}$  while the outer circle is the boundary of the C2 occulter at  $2.2 R_{\odot}$ .

Fig. 7a.— MDI magnetogram data for AR 8210, which was the source region for the CME of 03 May 1998. This active region is the source of several other CMEs and flares (Table 3). The bottom panel shows the location of the overall active region on the solar disk, while the top panels show a closeup of the active region. The top panel shows that there are two regions of cancelling magnetic flux over a timescale of  $\sim 6$  hours before the initiation of the CME in EIT 195 Å data.

Fig. 7b.— Running difference EIT 195 Å images that show the development of the CME of 03 May 1998. Contours of the photospheric magnetic field from MDI data are superimposed. The yellow contours denote +50 gauss fields and the green contours -50 gauss fields.

Fig. 7c.— Running difference images from the LASCO C2 coronagraph showing the development of the CME of 03 May 1998. The inner white circle in the center is at  $1 R_{\odot}$  while the outer circle is the boundary of the C2 occulter at  $2.2 R_{\odot}$ .

Fig. 8a.— MDI magnetogram data for 19 May 1998. The prominence is embedded in the weak fields to the west of the dominant active region.

Fig. 8b.— Running difference EIT 195 Å images that show the prominence eruption of 19 May 1998. Contours of the photospheric magnetic field from MDI data are superimposed. The red contours denote +10 gauss fields, blue -10 gauss, yellow +50 gauss and green -50 gauss.

Fig. 8c.— Straight EIT 195 Å images showing the prominence eruption of 19 May 1998.

Fig. 8d.— White light images from the LASCO C2 coronagraph showing the development of the CME of 19 May 1998. The prominence is clearly evident in the right panel. The inner white circle in the center is at  $1 R_{\odot}$  while the outer circle is the boundary of the C2 occulter at  $2.2 R_{\odot}$ .

Table 1. Catalog of all CMEs used in this study

Date	Initiation time (UT) <sup>1</sup>	Category
97/04/01	13:46	AR <sup>3</sup>
97/10/10	03:45	AR
97/10/11	08:51	AR
97/11/04	05:58	AR
97/11/06	11:41	AR
98/01/08	08:59	AR
98/01/17	23:36	AR
98/01/20	21:05	AR <sup>3</sup>
98/01/27	22:20	AR
98/04/27	08:51	AR <sup>2</sup>
98/05/06	07:59	AR <sup>2</sup>
98/05/27	11:19	AR
98/06/08	16:04	AR
96/12/23	20:20	AR+EP
97/04/07	14:00	AR+EP
97/05/12	04:50	AR+(EP) <sup>4</sup>
97/10/13	08:34	AR+EP
97/10/21	17:34	AR+EP
97/11/27	13:12	AR+(EP) <sup>4</sup>
98/01/25	14:32	AR+EP <sup>3</sup>
98/01/26	23:05	AR+(EP) <sup>4</sup>
98/03/27	00:45	AR+(EP) <sup>4</sup>
98/04/15	07:14	AR+EP
98/04/29	15:52	AR+EP
98/05/02	13:21	AR+(EP) <sup>2,4</sup>

Table 1—Continued

Date	Initiation time (UT) <sup>1</sup>	Category
98/05/03	21:12	AR+EP <sup>2,3</sup>
98/05/05	23:36	AR+EP <sup>2</sup>
96/10/19	15:00	EP
97/10/06	14:10	EP
97/10/21	00:20	EP <sup>3</sup>
98/01/21	06:43	EP
98/05/19	07:54	EP <sup>3</sup>

<sup>1</sup>Initiation time as discerned from the source region in EIT 195 Å data

<sup>2</sup>Events associated with NOAA active region 8210

<sup>3</sup>Case studies examined in detail (§3.2)

<sup>4</sup>Evidence for an erupting prominence is not very strong

Table 2. CMEs used for detailed case studies

CME	Category	Flare	AR lifetime	AR phase	Short Timescale Behavior ( $\sim 6$ hrs)
97/04/01	AR	M1.9	53-75 days	Rising phase	Parasitic polarity forms lane
97/10/21	AR+P	C3.3	$\sim 6$ months	Decaying	None
98/01/20	AR	None	11-36 days	Mid-life	Cancelling flux
98/01/25	AR+P	C1.1	$\sim 7$ months	Decaying	None
98/05/03 <sup>1</sup>	AR	M1.4	$\sim 65-79$ days	Mid-life	Cancelling flux

<sup>1</sup>Prolific active region, see Table 3



Table 3. Events associated with NOAA active region 8210

Date	CME in C2 (UT)	Flare peak time (UT)	Flare class
98/04/27	09:26	09:20	X1.0
98/05/02	14:06	13:42	X1.1
98/05/03	21:31	21:29	M1.4
98/05/06	00:02	23:46 (05/05)	M2.5
98/05/06	08:04	08:09	X2.7

**Contents**

<b>1</b>	<b>Introduction</b>	<b>3</b>
<b>2</b>	<b>Data Analysis Procedure</b>	<b>5</b>
<b>3</b>	<b>Results</b>	<b>7</b>
3.1	Aggregate Results . . . . .	7
3.2	Case Studies . . . . .	10
3.2.1	The CME of 01 April 1997 . . . . .	10
3.2.2	The CME of 21 October 1997 . . . . .	13
3.2.3	The CME of 20 January 1998 . . . . .	15
3.2.4	The CME of 25 January 1998 . . . . .	16
3.2.5	The CME of 03 May 1998 . . . . .	18
3.2.6	The CME of 19 May 1998 . . . . .	20
<b>4</b>	<b>Discussion and Conclusions</b>	<b>20</b>

### List of Figures

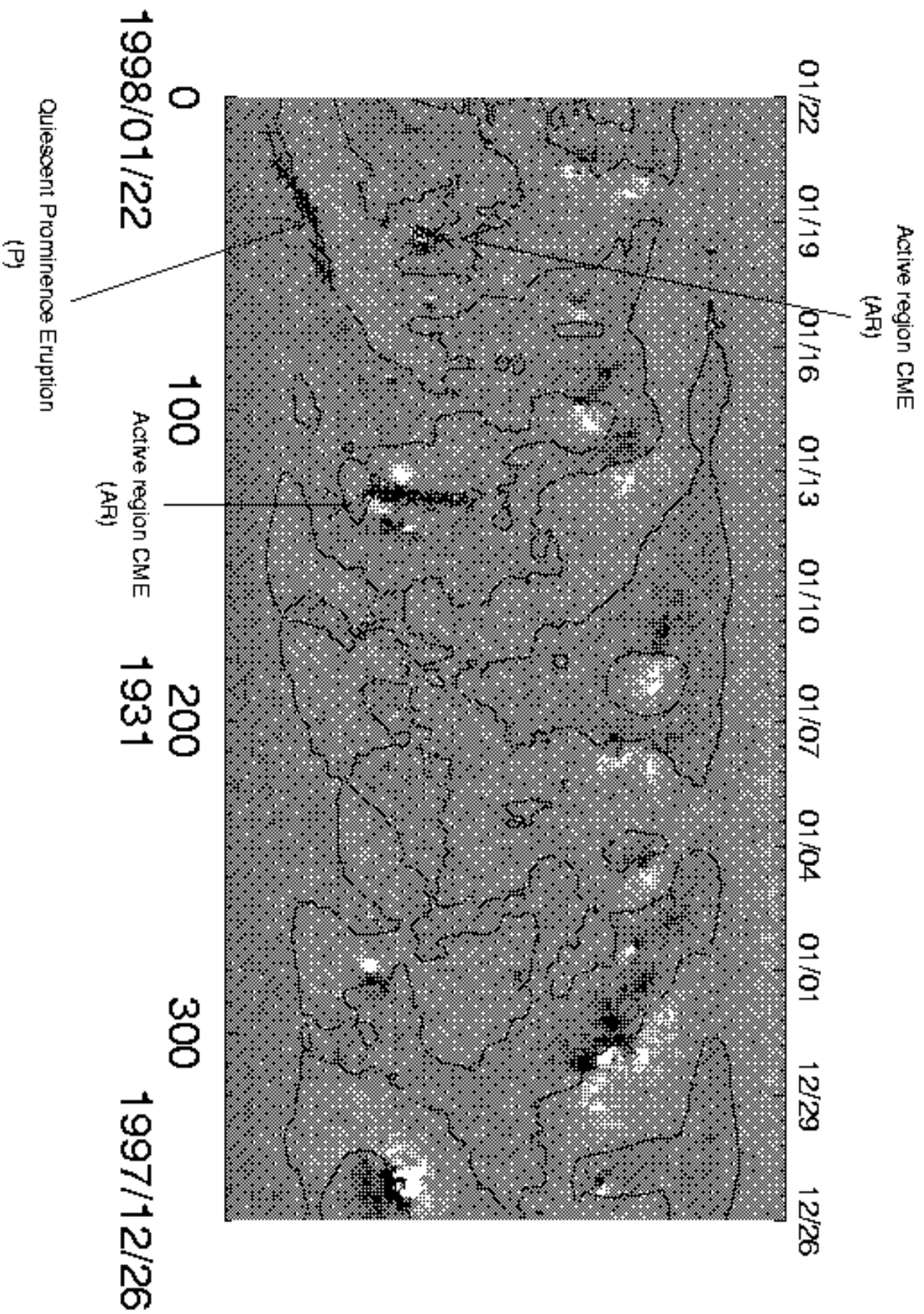
1a	The background is the synoptic magnetogram from the Kitt Peak NSO for Carrington rotation 1931. The on-disk CMEs observed in EIT 195 Å data during this rotation are superimposed on the magnetogram. . . . .	25
1b	The background is the synoptic magnetogram from the Kitt Peak NSO for Carrington rotation 1932. The on-disk CMEs observed in EIT 195 Å data during this rotation are superimposed on the magnetogram. We have examined such magnetograms for rotations 1915-1935. We show only two examples here in order to conserve space. . . . .	25
2	This figure gives the number of on-disk CMEs in each of the categories AR, AR+EP and EP. Of the 32 on-disk CMEs recorded in EIT 195 Å data, 13 are associated with active regions (AR), 5 with eruptions of prominences outside active regions (EP) and 14 with eruptions of active region prominences (AR+EP). . . . .	25
3a	MDI magnetogram data for AR 8026, which was the source region for the CME of 01 April 1997. The bottom panel shows the location of the overall active region on the solar disk, while the top panels show a closeup of the active region. The parasitic negative polarity (marked by the black arrow on the top panels) grows over a timescale of $\sim 6$ hours near the CME initiation time to form a lane in the midst of the positive polarity region. The CME starts developing on the disk as seen in EIT 195 Å images around 13:46 UT, and the parasitic polarity continues to grow and form the lane well beyond 14:27 UT. . . . .	25

3b	Running difference EIT 195 Å images that show the development of the CME of 01 April 1997. Contours of the photospheric magnetic field from MDI data are superimposed. The red contours denote +10 gauss fields, yellow +50 gauss, blue -10 gauss and green -50 gauss. . . . .	25
3c	Straight EIT 195 Å image showing part of the flare associated with the CME of 01 April 1997. Contours of the photospheric magnetic field from MDI data are superimposed. The red contours denote +10 gauss fields, blue -10 gauss, yellow +50 gauss and green -50 gauss. It can be seen that the flare occurs at the location of the parasitic negative polarity. . . . .	26
3d	Running difference images from the LASCO C2 coronagraph showing the development of the CME of 01 April 1997. The inner white circle in the center is at $1 R_{\odot}$ while the outer circle is the boundary of the C2 occulter at $2.2 R_{\odot}$ . . . . .	26
4a	MDI magnetogram data showing AR 8907 and the associated decaying active region complex to its northeast. The CME of 21 October 1997 was associated with the eruption of a filament above the neutral line of the decaying active region complex. . . . .	26
4b	Running difference EIT 195 Å images that show the development of the CME of 21 Oct 1997. Contours of the photospheric magnetic field from MDI data are superimposed. The red contours denote +10 gauss fields, blue -10 gauss, yellow +50 gauss and green -50 gauss. . . . .	26

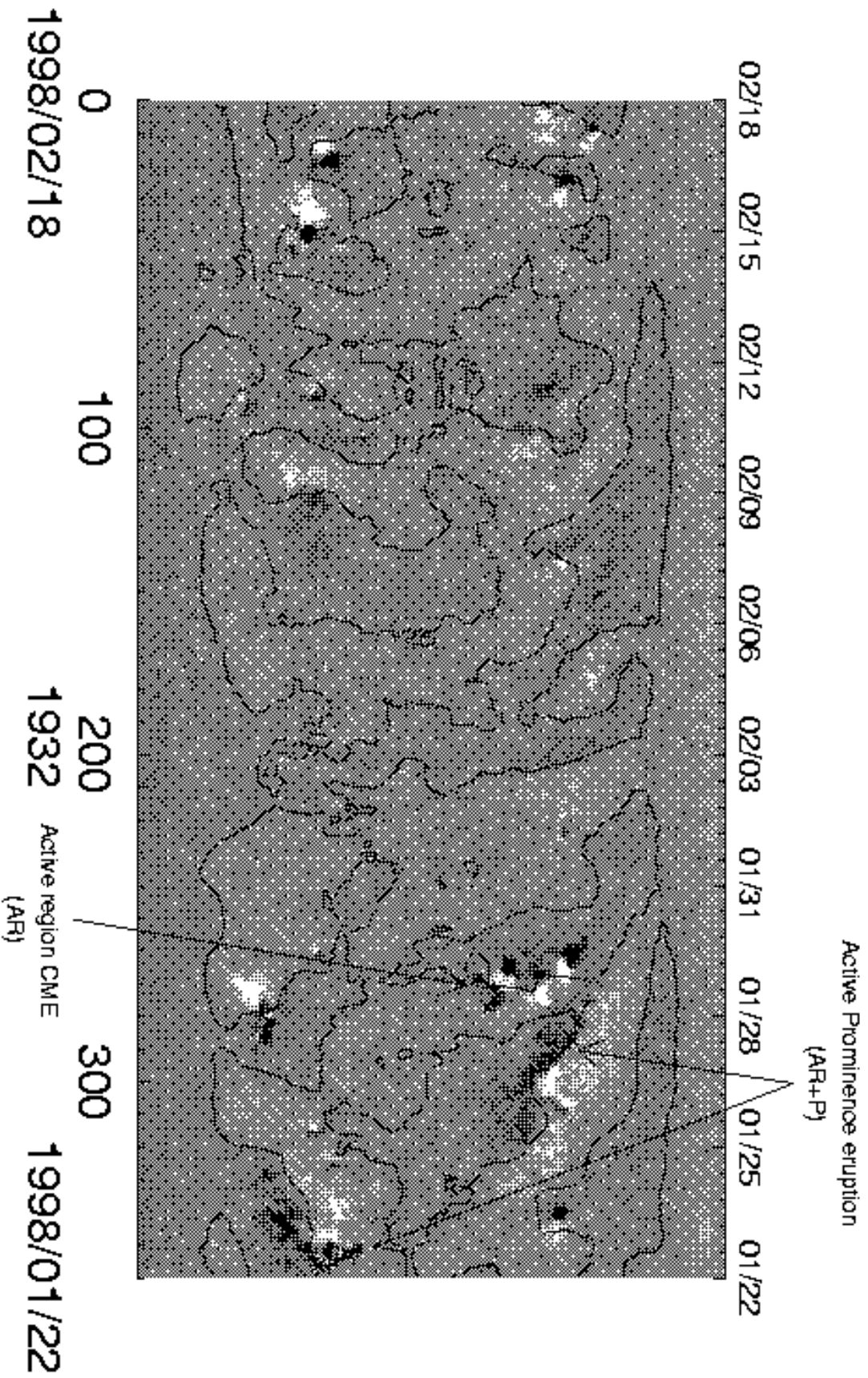
4c	Straight EIT 195 Å images showing the flaring activity associated with the CME of 21 Oct 1997. The twin ribbon configuration evident in the lower panel is of special interest. Contours of the photospheric magnetic field from MDI data are superimposed. The yellow contours denote +50 gauss fields and the green contours -50 gauss fields. . . . .	26
4d	Running difference images from the LASCO C2 coronagraph showing the development of the CME of 21 Oct 1997. The inner white circle in the center is at $1 R_{\odot}$ while the outer circle is the boundary of the C2 occulter at $2.2 R_{\odot}$ .	26
5a	MDI magnetogram data for AR 8135, which was the source region for the CME of 20 Jan 1998. The bottom panel shows the location of the overall active region on the solar disk, while the top panels show a closeup of the active region. The top panels show flux cancellation near the area marked by the white arrows over a $\sim 6$ hour timescale before the initiation of the CME in EIT 195 Å data. . . . .	27
5b	Running difference EIT 195 Å images that show the development of the CME of 20 Jan 1998. Contours of the photospheric magnetic field from MDI data are superimposed. The red contours denote +10 gauss fields, blue -10 gauss, yellow +50 gauss and green -50 gauss. . . . .	27
5c	Running difference images from the LASCO C2 coronagraph showing the development of the CME of 20 Jan 1998. The inner white circle in the center is at $1 R_{\odot}$ while the outer circle is the boundary of the C2 occulter at $2.2 R_{\odot}$ .	27

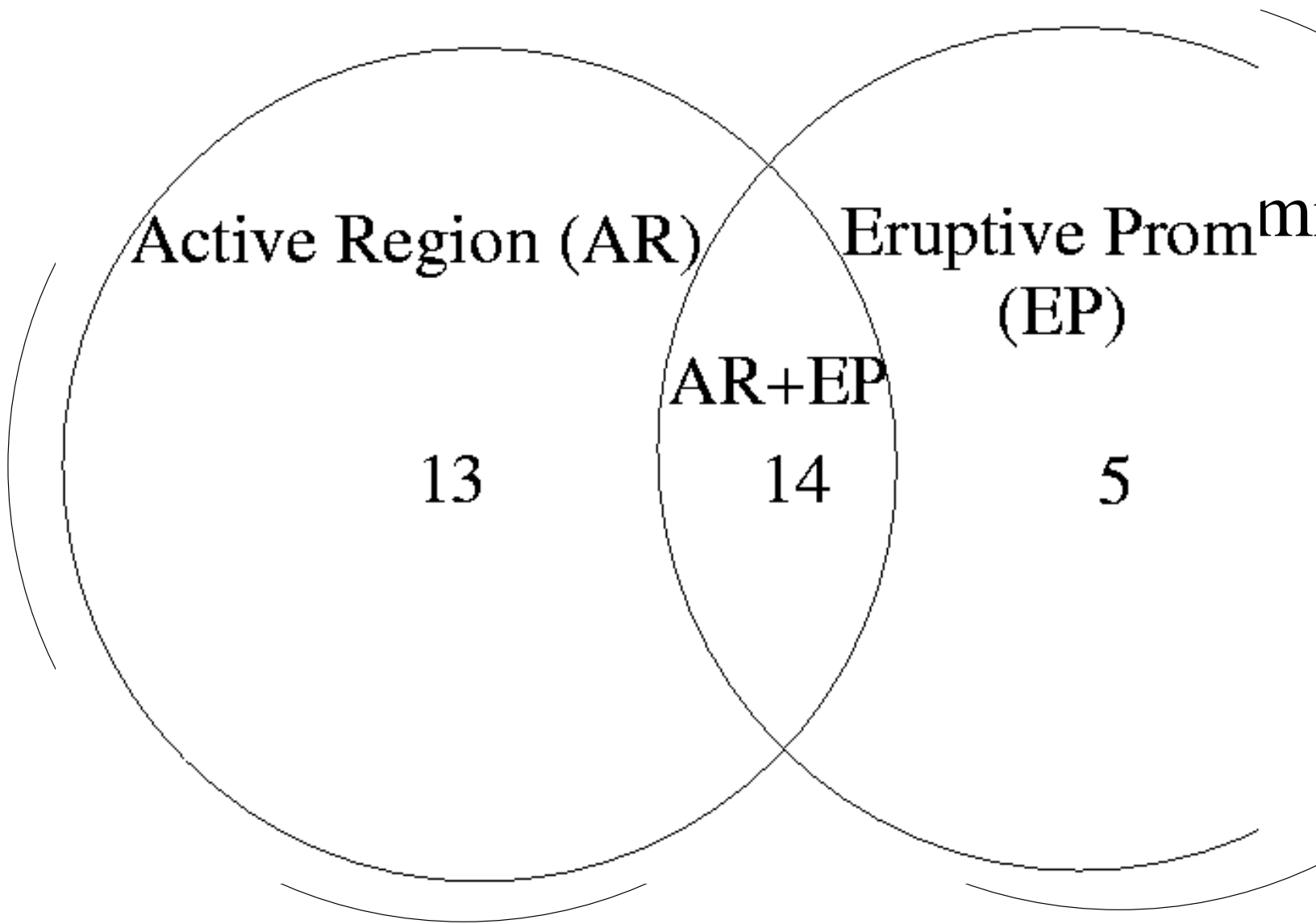
6a	MDI magnetogram data showing AR 8145 and the associated decaying active region complex to its west. The CME of 25 Jan 1998 was associated with the eruption of a filament above the neutral line of the decaying active region complex. . . . .	27
6b	Running difference EIT 195 Å images that show the development of the CME of 25 Jan 1998. Contours of the photospheric magnetic field from MDI data are superimposed. The red contours denote +10 gauss fields, blue -10 gauss, yellow +50 gauss and green -50 gauss. . . . .	27
6c	Running difference EIT 195 Å images that show the latter stages of development of the CME of 25 Jan 1998. . . . .	27
6d	Running difference images from the LASCO C2 coronagraph showing the development of the CME of 25 Jan 1998. The inner white circle in the center is at $1 R_{\odot}$ while the outer circle is the boundary of the C2 occulter at $2.2 R_{\odot}$ . . . . .	28
7a	MDI magnetogram data for AR 8210, which was the source region for the CME of 03 May 1998. This active region is the source of several other CMEs and flares (Table 3). The bottom panel shows the location of the overall active region on the solar disk, while the top panels show a closeup of the active region. The top panel shows that there are two regions of cancelling magnetic flux over a timescale of $\sim 6$ hours before the initiation of the CME in EIT 195 Å data. . . . .	28
7b	Running difference EIT 195 Å images that show the development of the CME of 03 May 1998. Contours of the photospheric magnetic field from MDI data are superimposed. The yellow contours denote +50 gauss fields and the green contours -50 gauss fields. . . . .	28

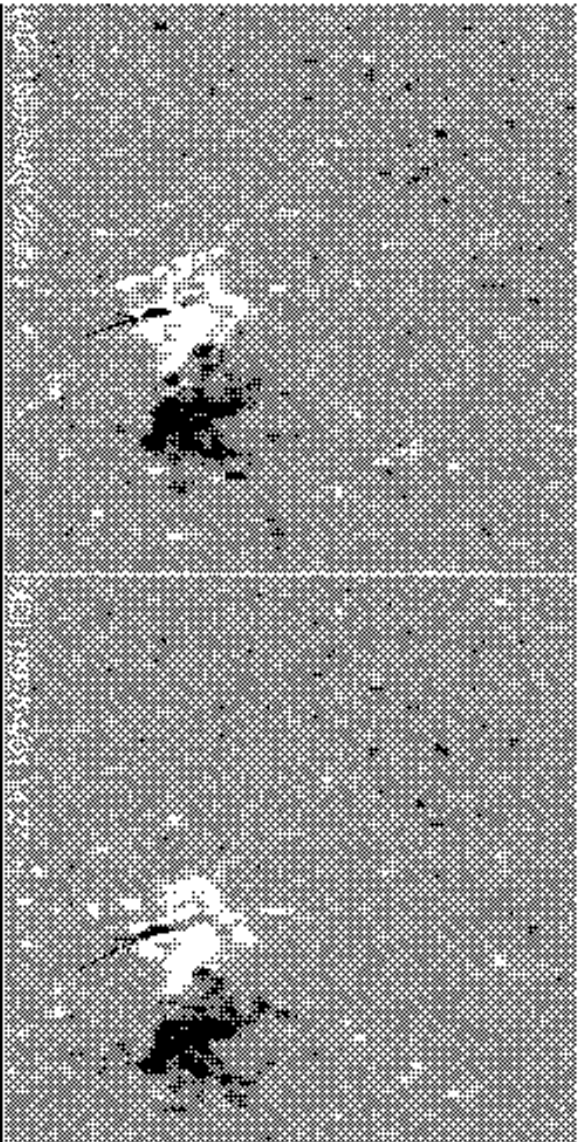
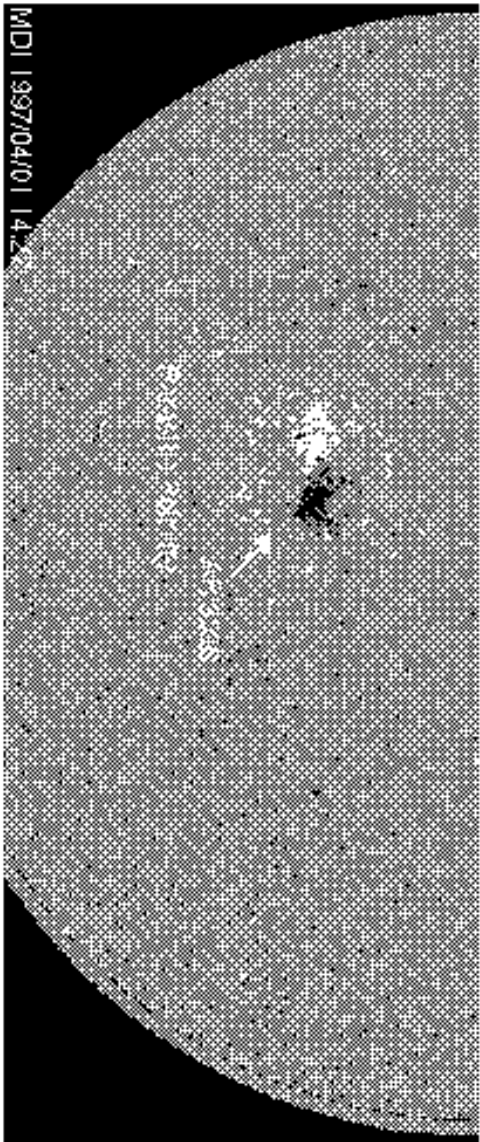
7c	Running difference images from the LASCO C2 coronagraph showing the development of the CME of 03 May 1998. The inner white circle in the center is at $1 R_{\odot}$ while the outer circle is the boundary of the C2 occulter at $2.2 R_{\odot}$ .	28
8a	MDI magnetogram data for 19 May 1998. The prominence is embedded in the weak fields to the west of the dominant active region. . . . .	28
8b	Running difference EIT 195 Å images that show the prominence eruption of 19 May 1998. Contours of the photospheric magnetic field from MDI data are superimposed. The red contours denote +10 gauss fields, blue -10 gauss, yellow +50 gauss and green -50 gauss. . . . .	28
8c	Straight EIT 195 Å images showing the prominence eruption of 19 May 1998.	29
8d	White light images from the LASCO C2 coronagraph showing the development of the CME of 19 May 1998. The prominence is clearly evident in the right panel. The inner white circle in the center is at $1 R_{\odot}$ while the outer circle is the boundary of the C2 occulter at $2.2 R_{\odot}$ . . . . .	29









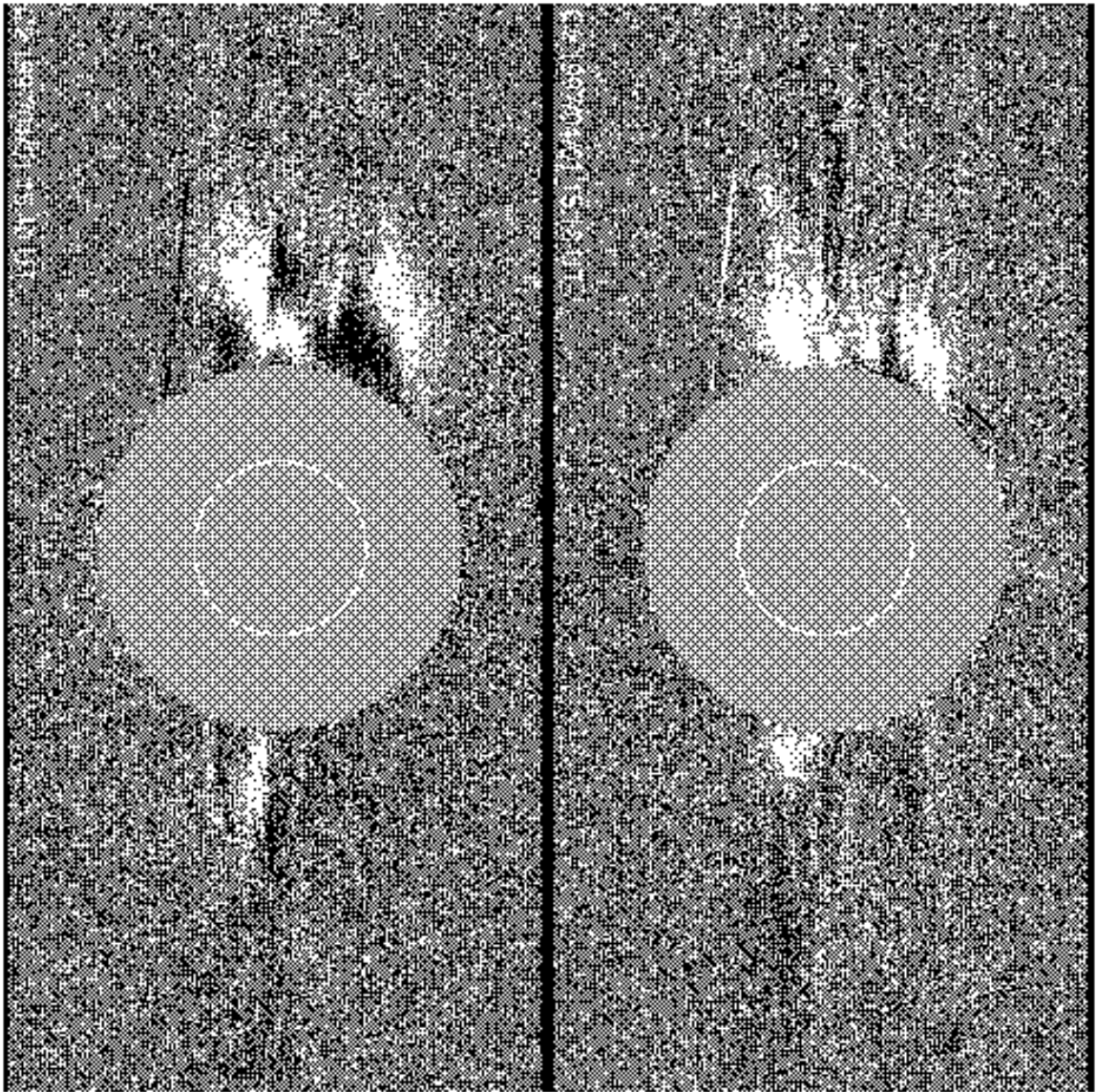




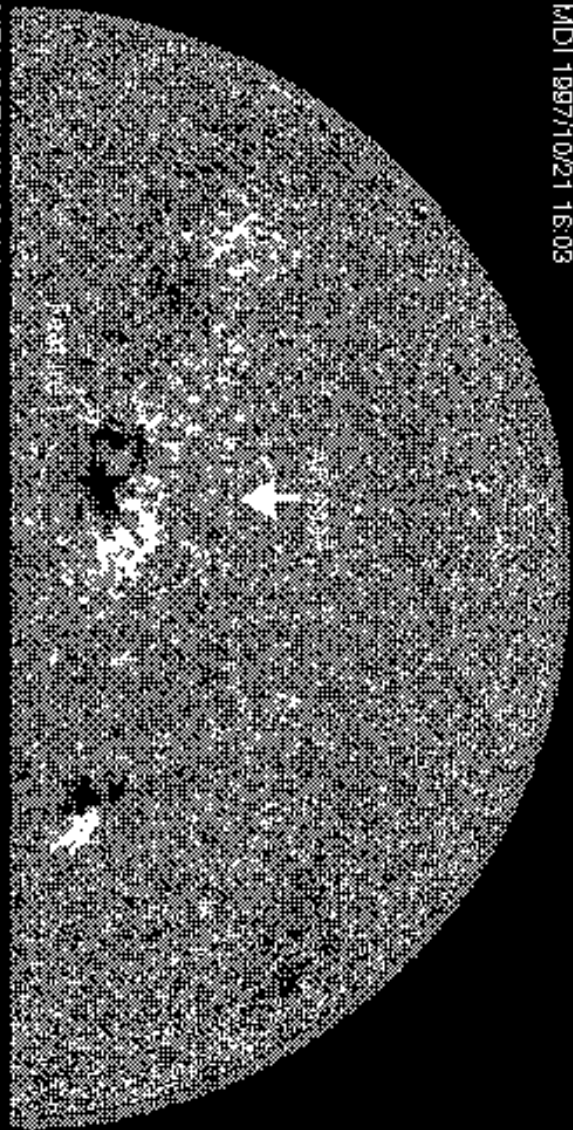
ET 1997/04/01 14:00  
MDI 1997/04/01 14:27

Parasitic Foamy Flare

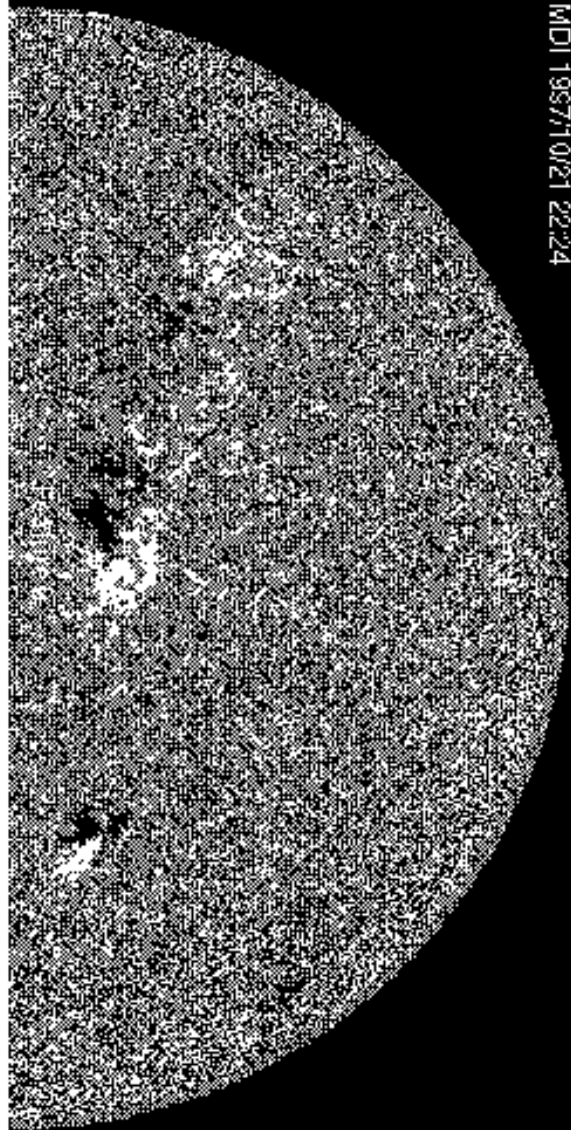


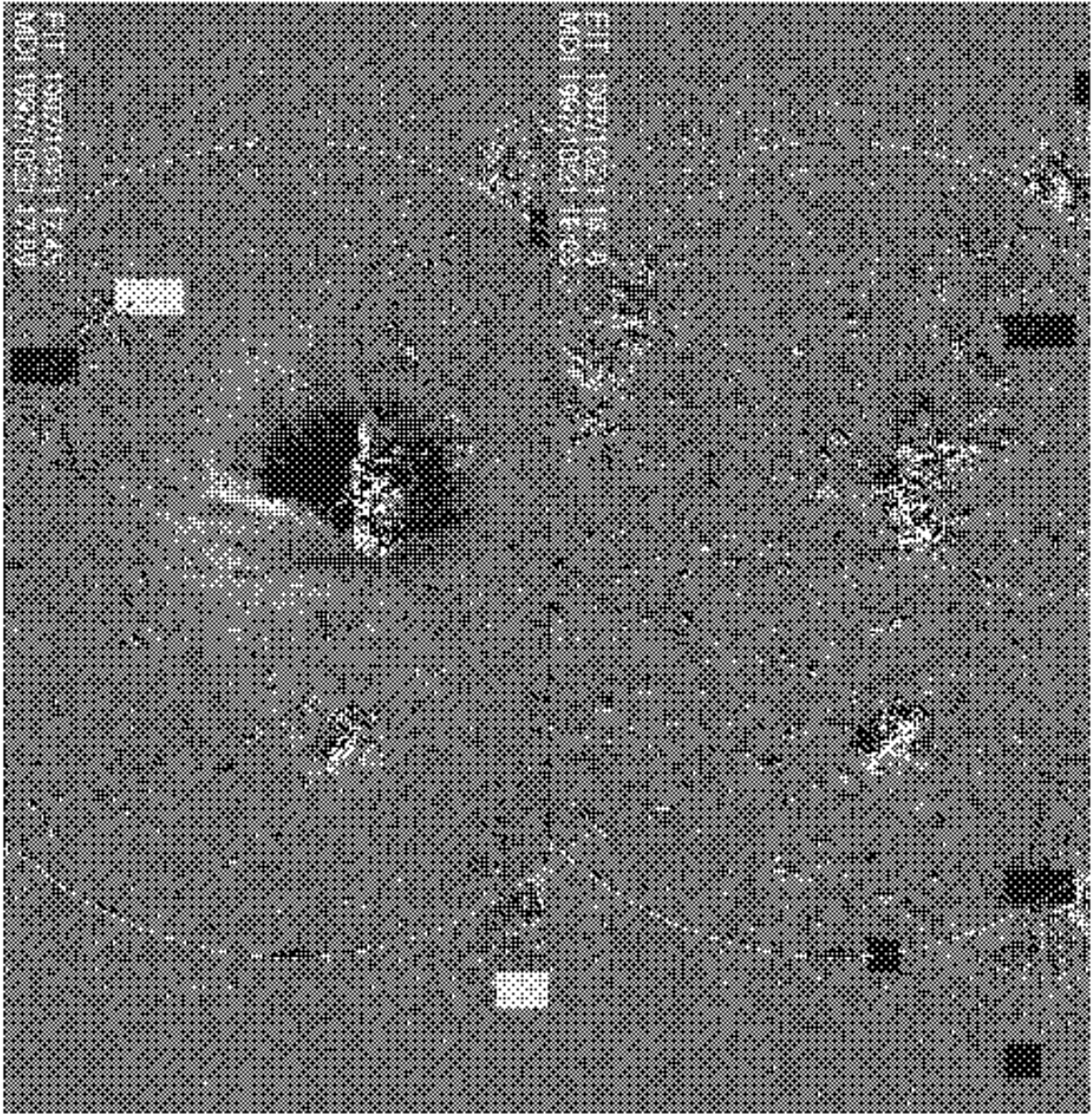


MDI 1997/10/21 16:03

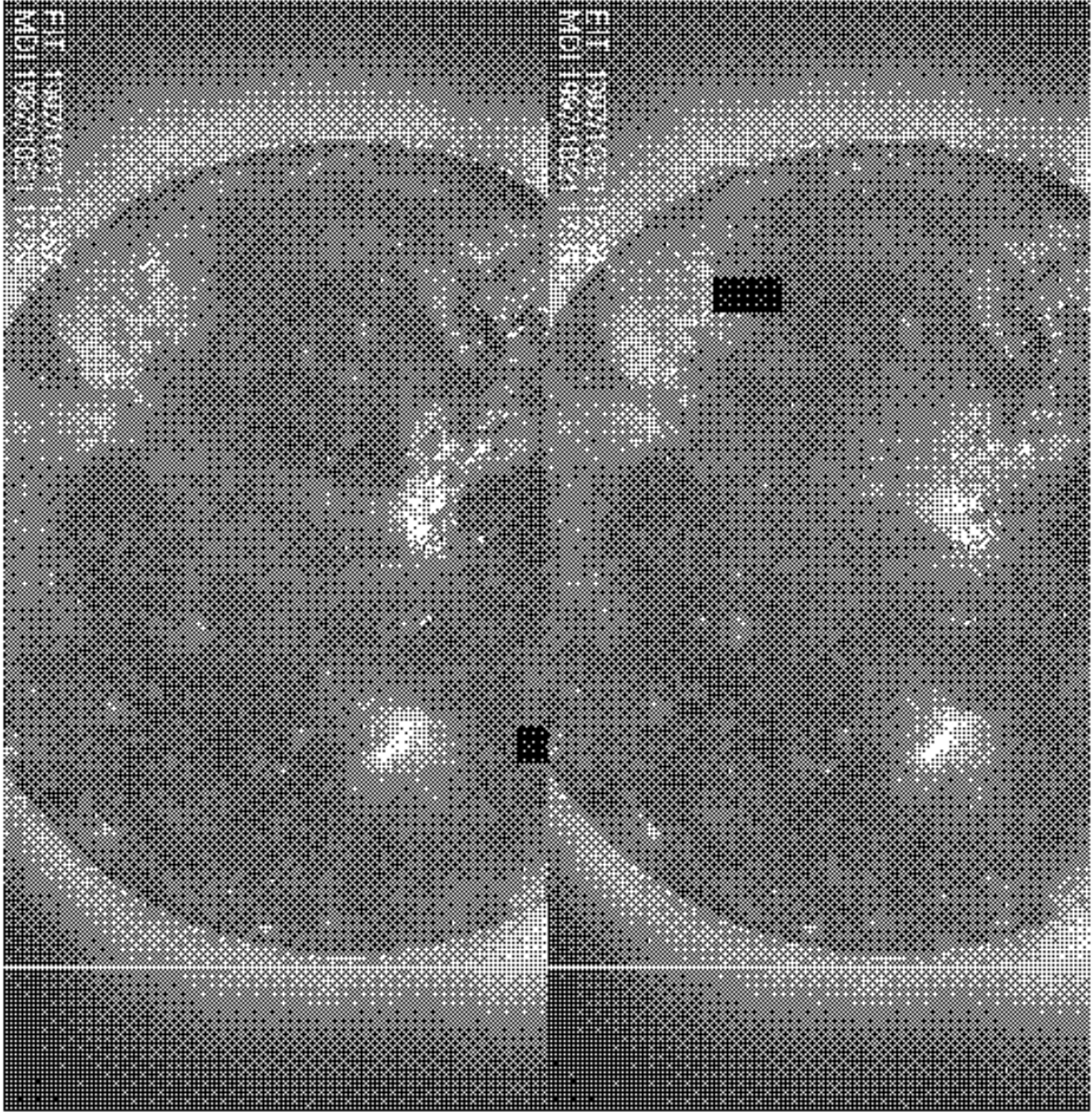


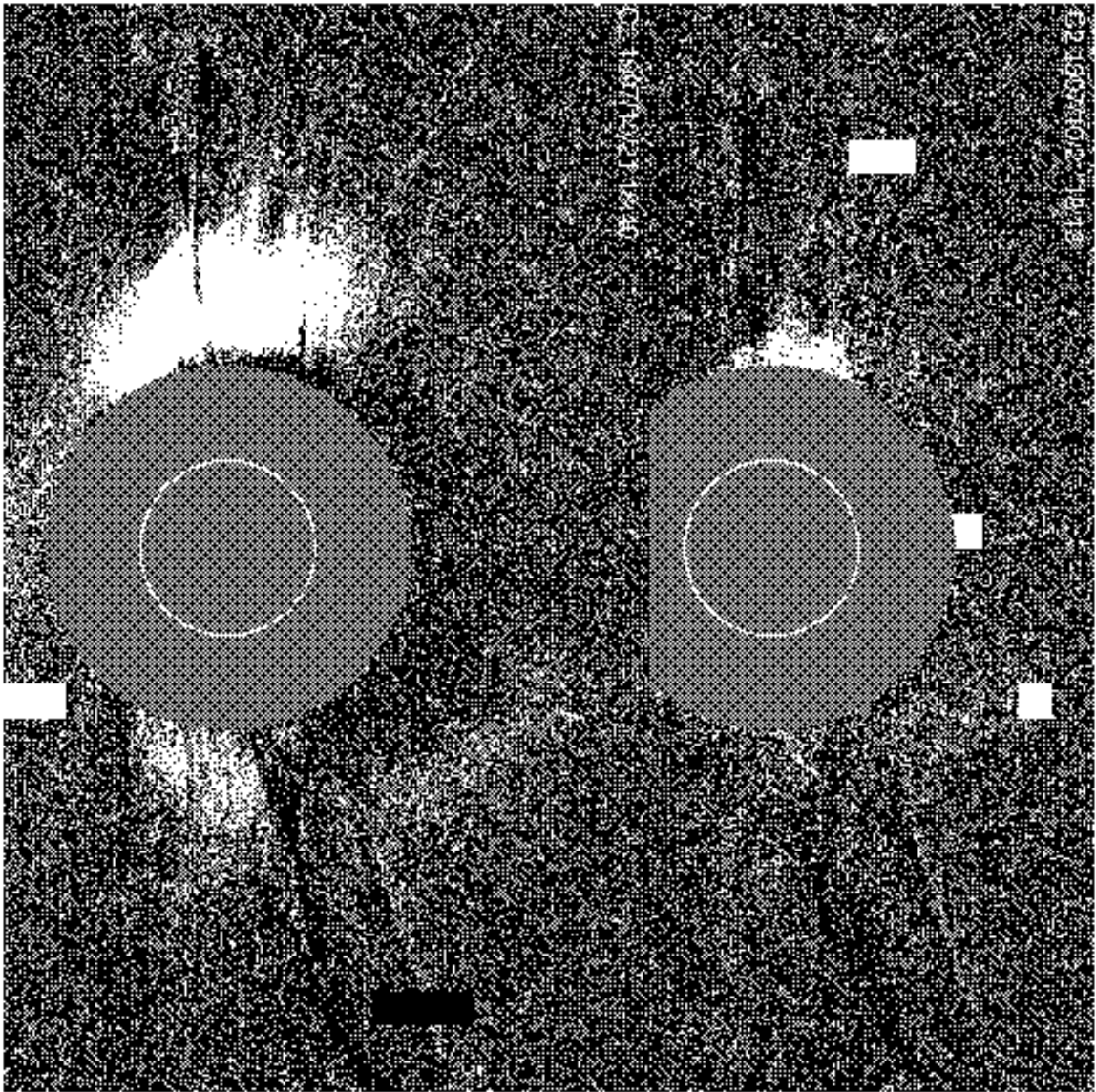
MDI 1997/10/21 22:24

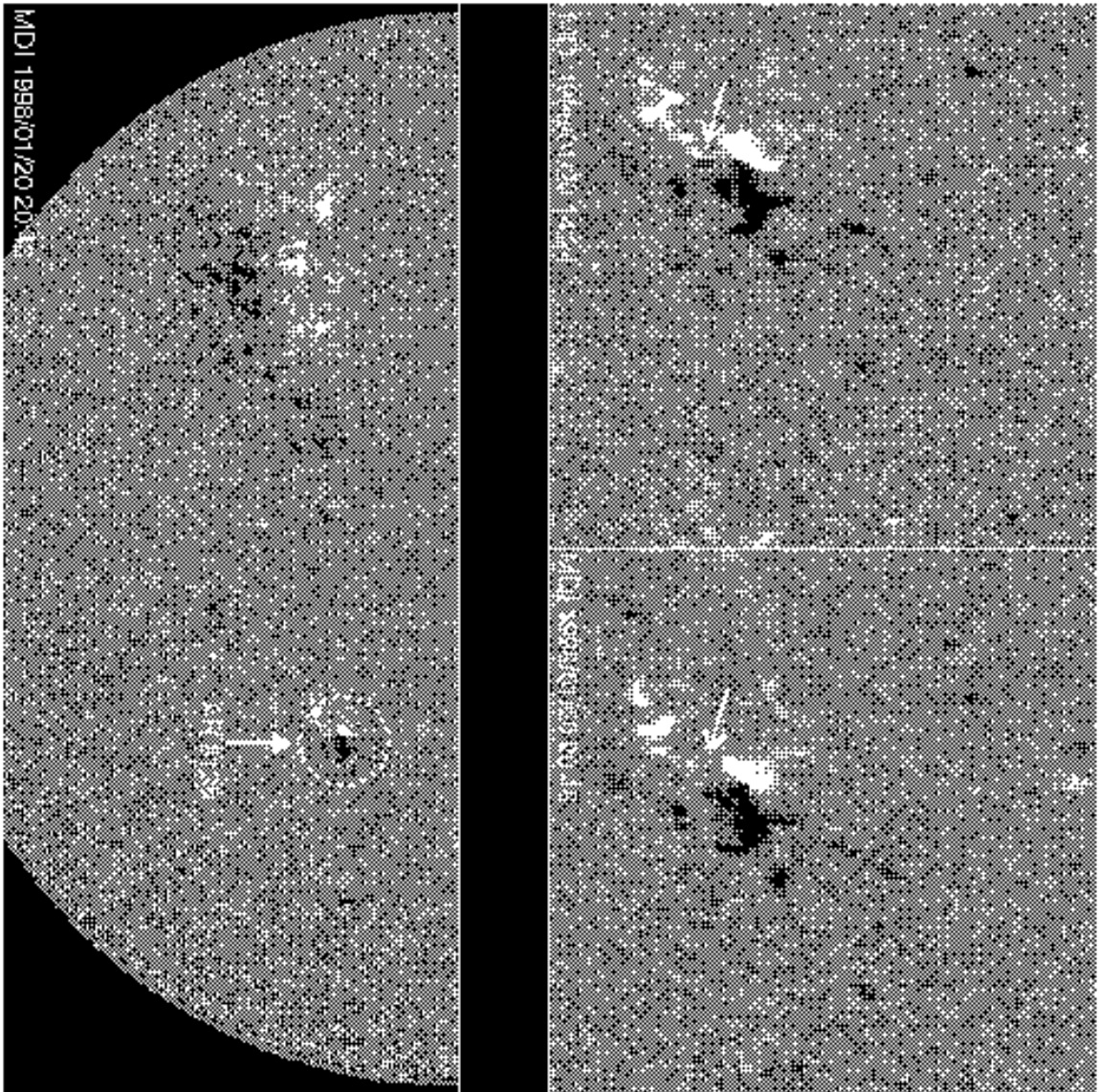


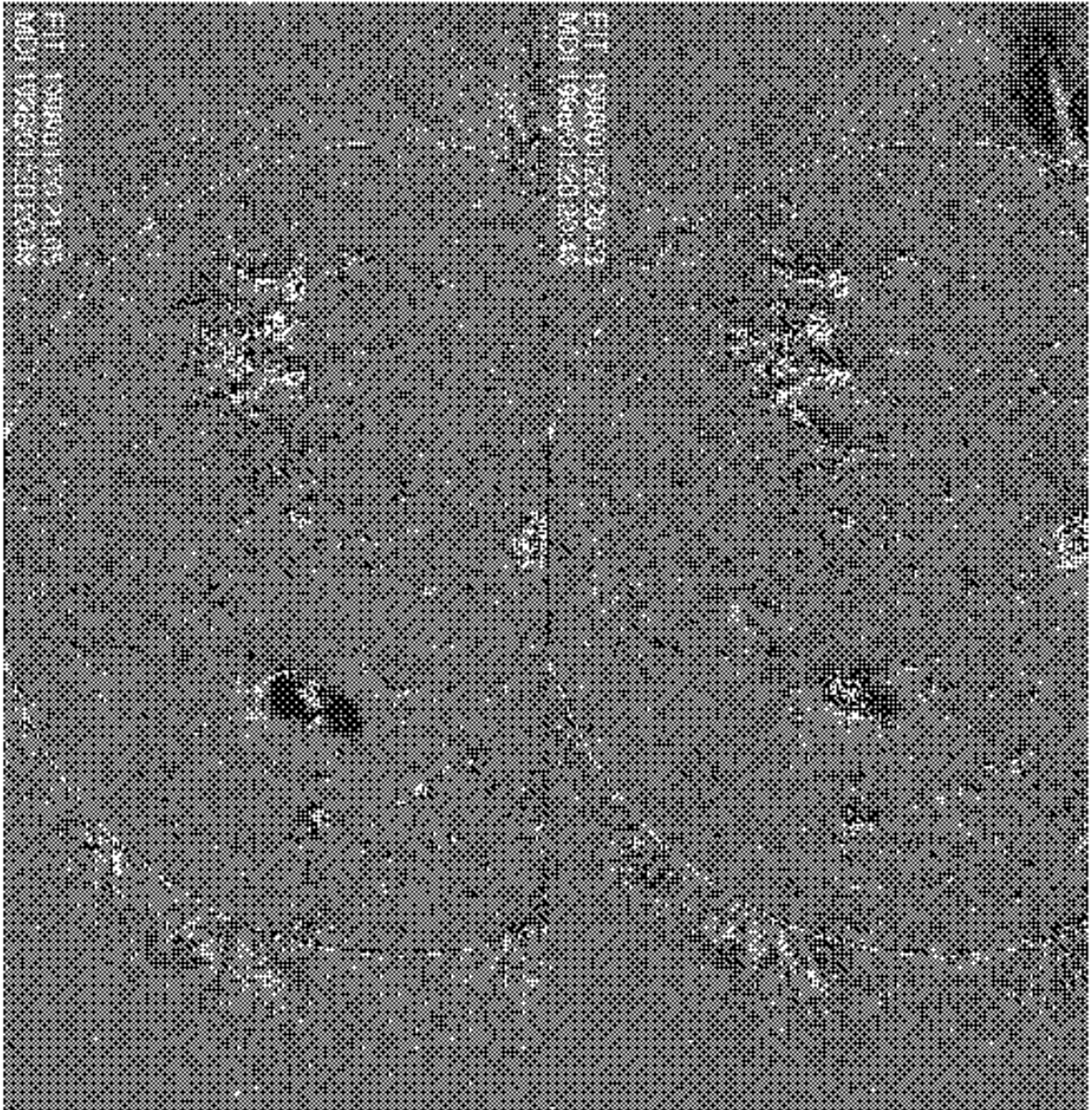


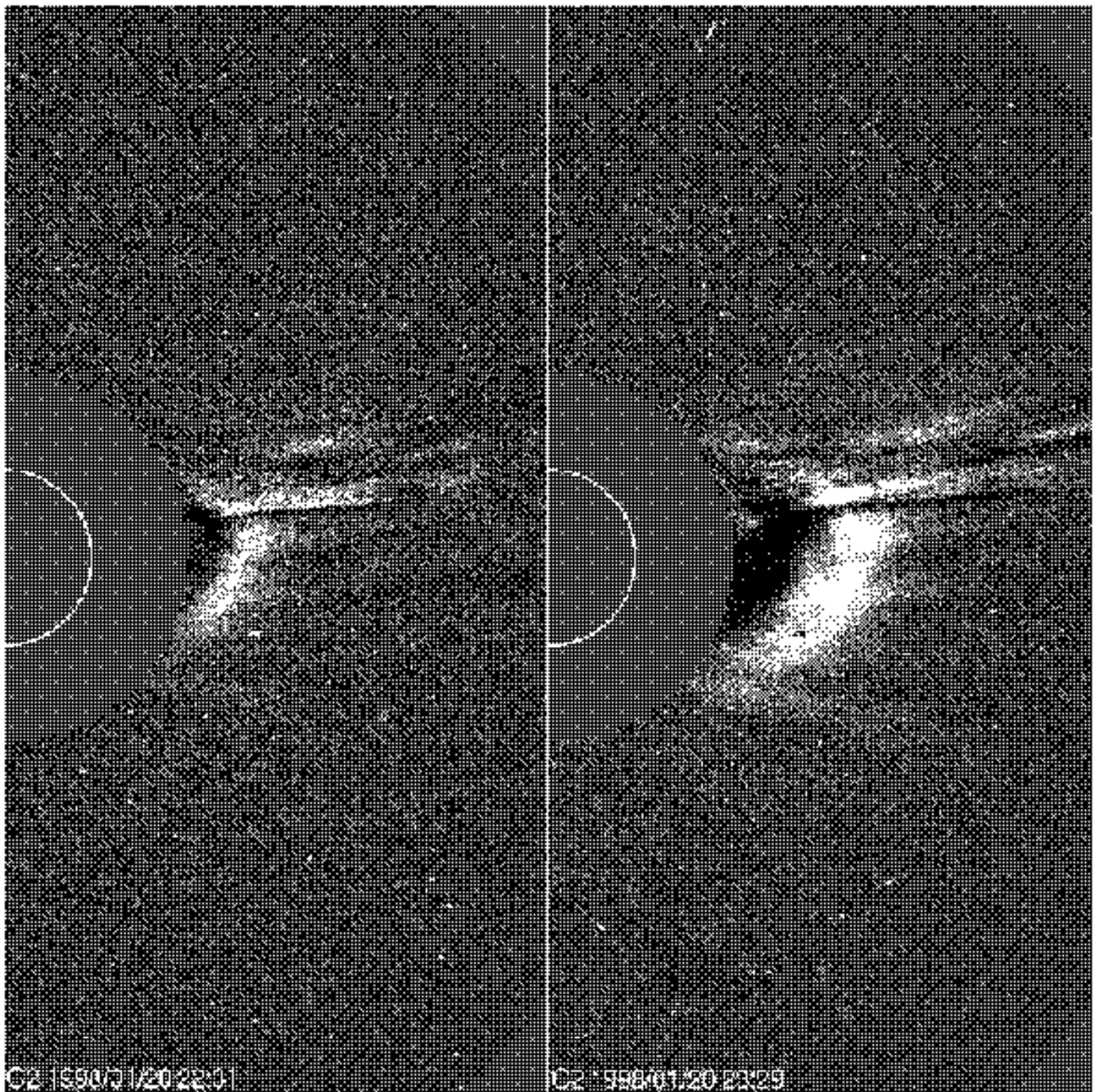








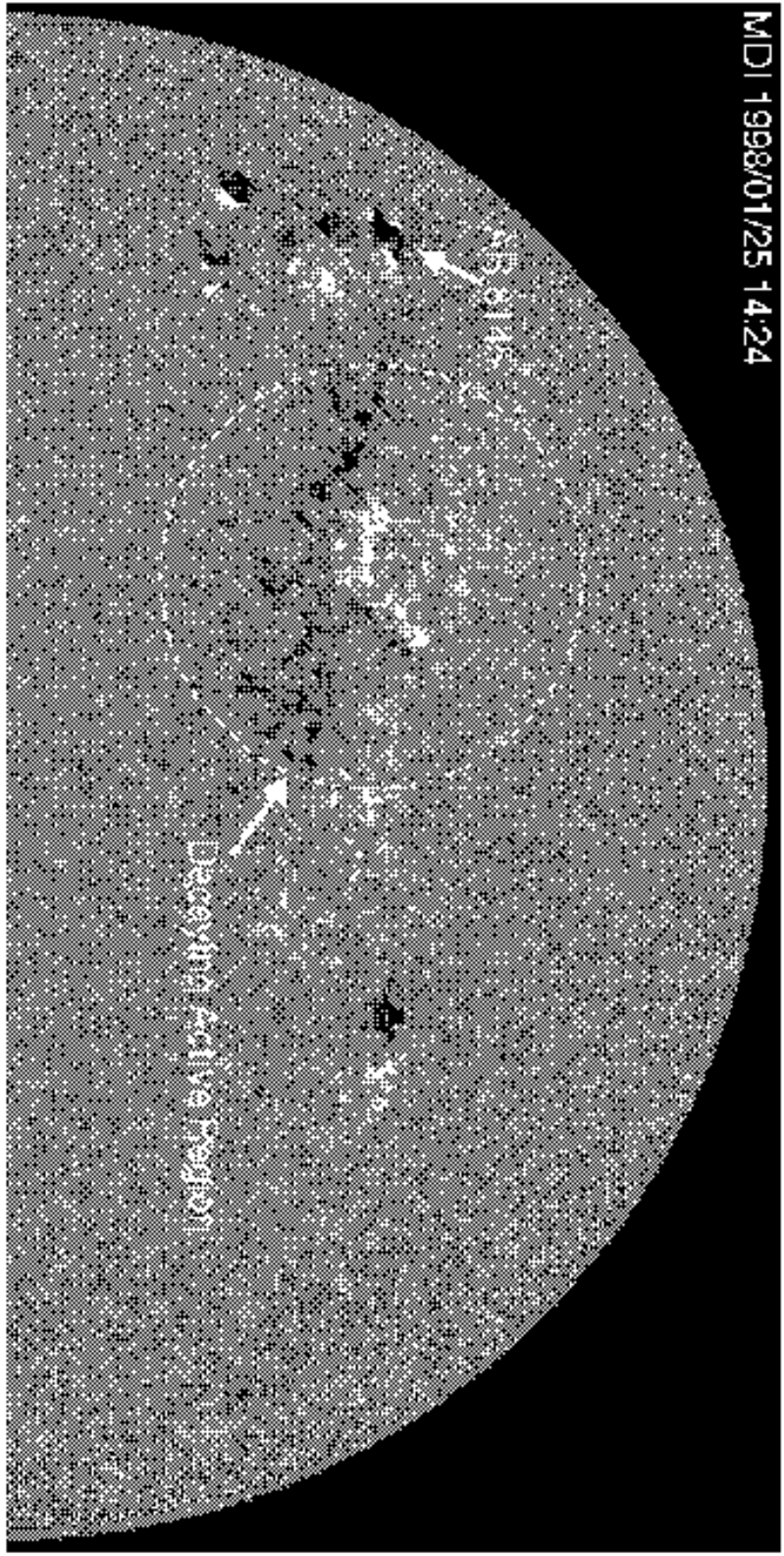


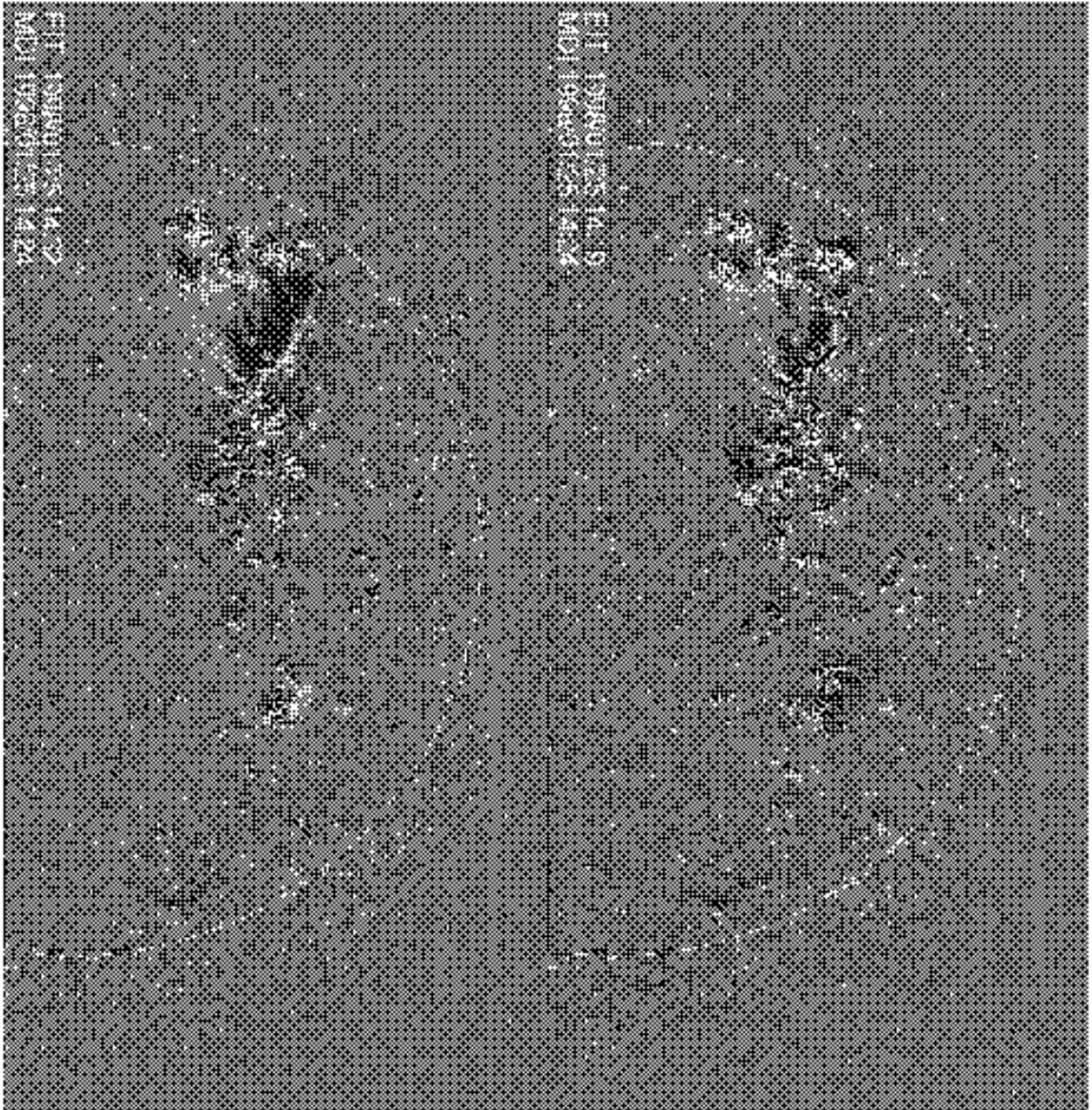


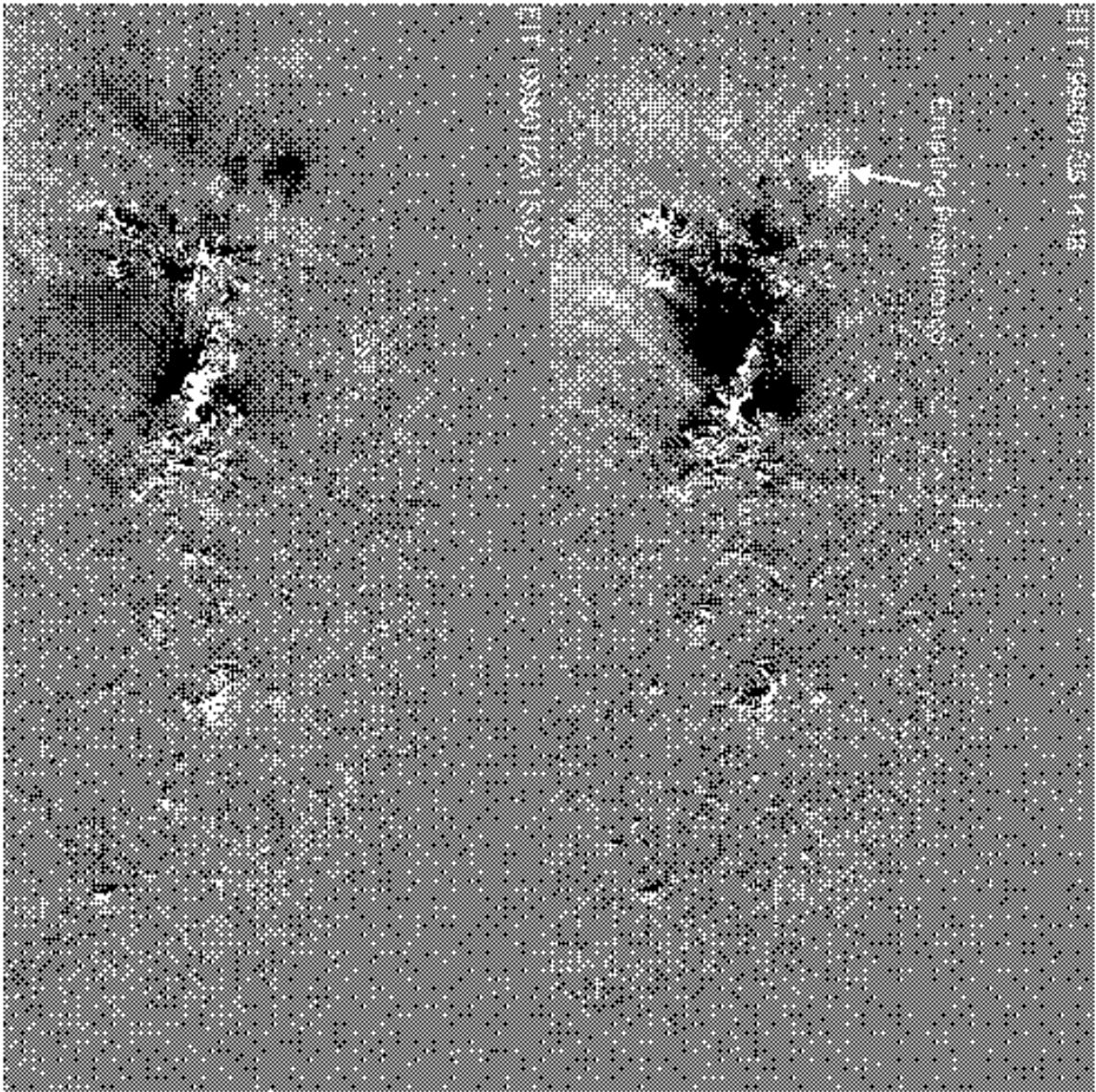
C2 1990/1/20 22:31

C2 1998/01/20 23:29

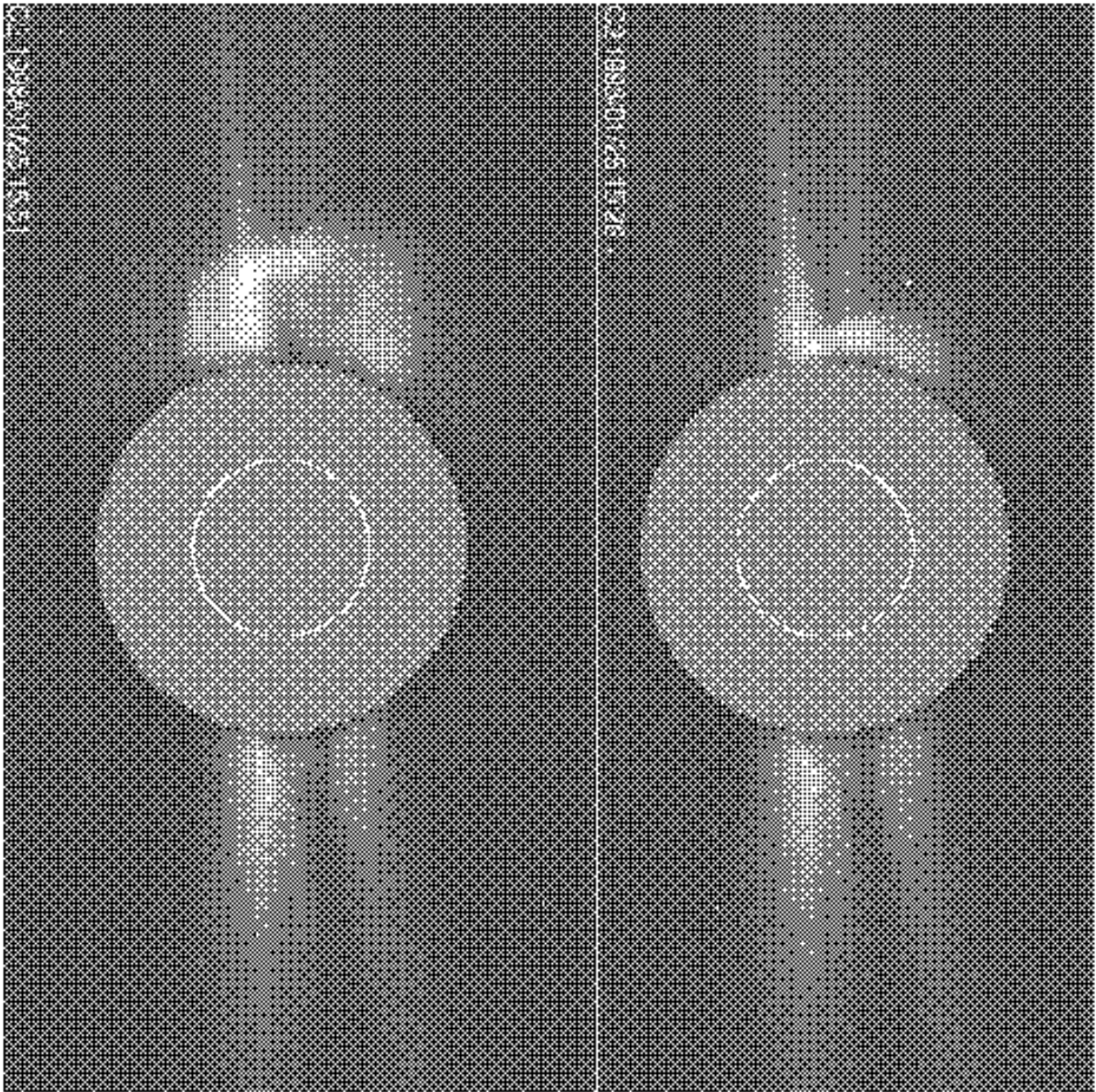
MIDI 1998/01/25 14:24

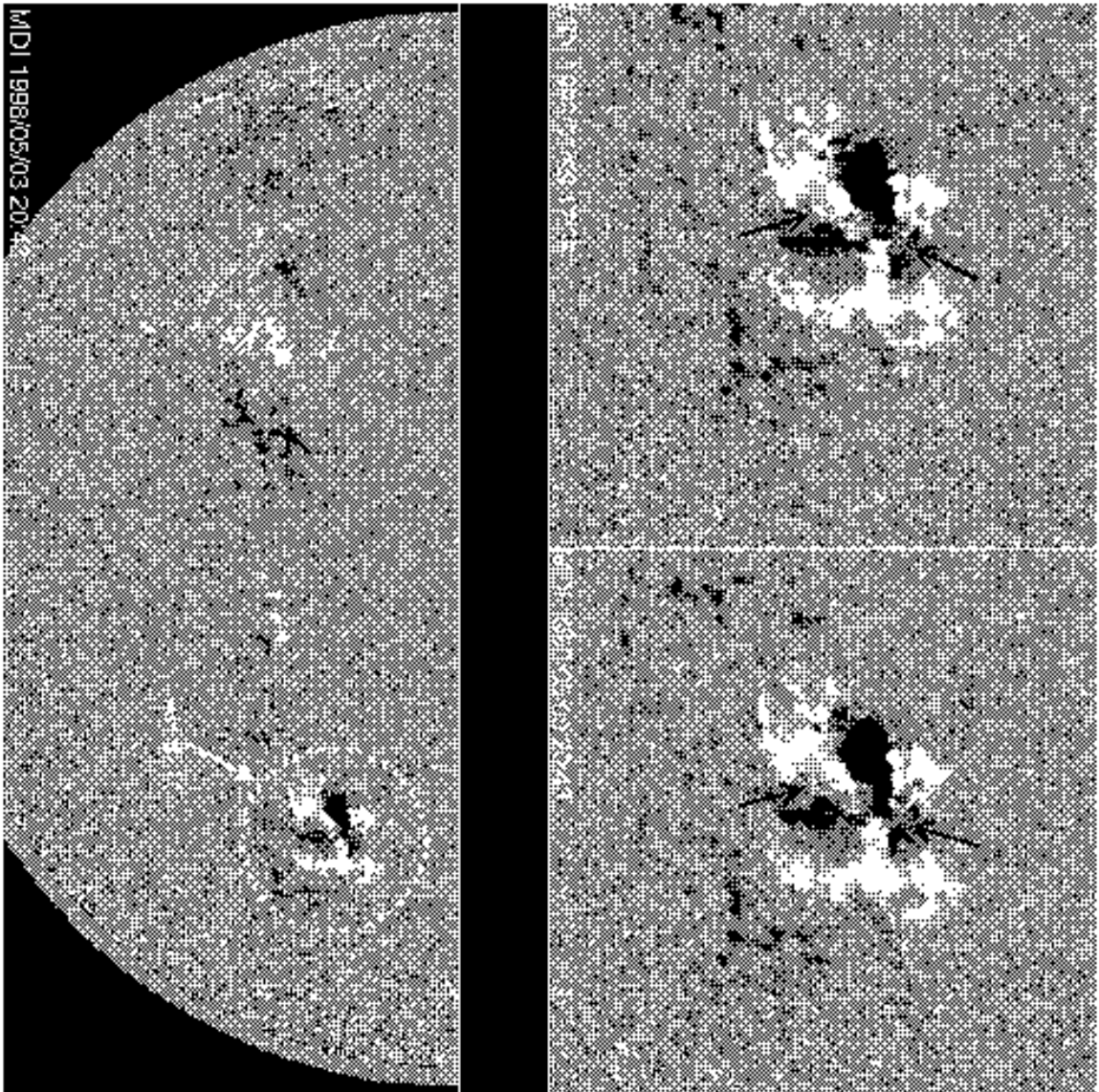


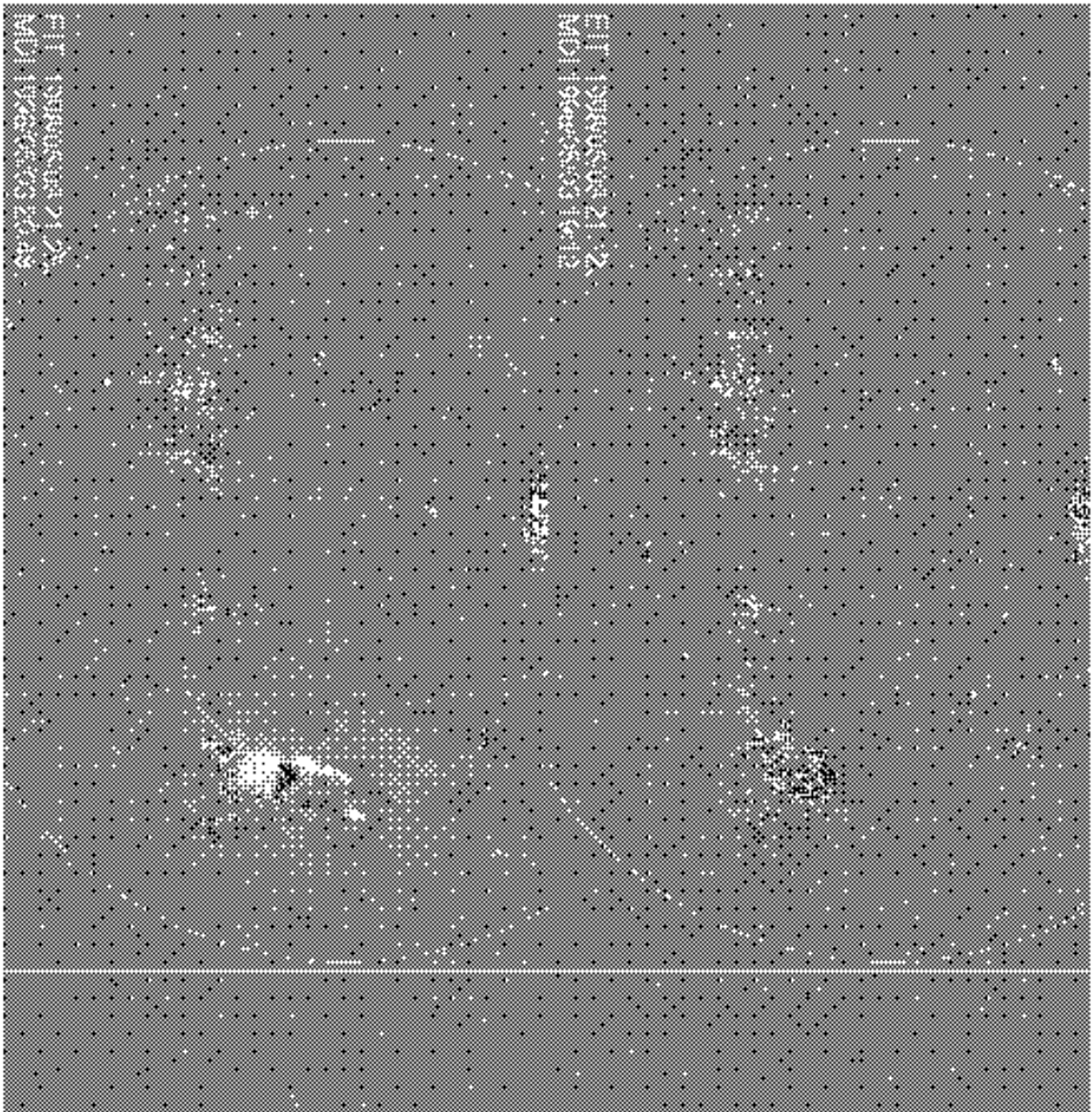


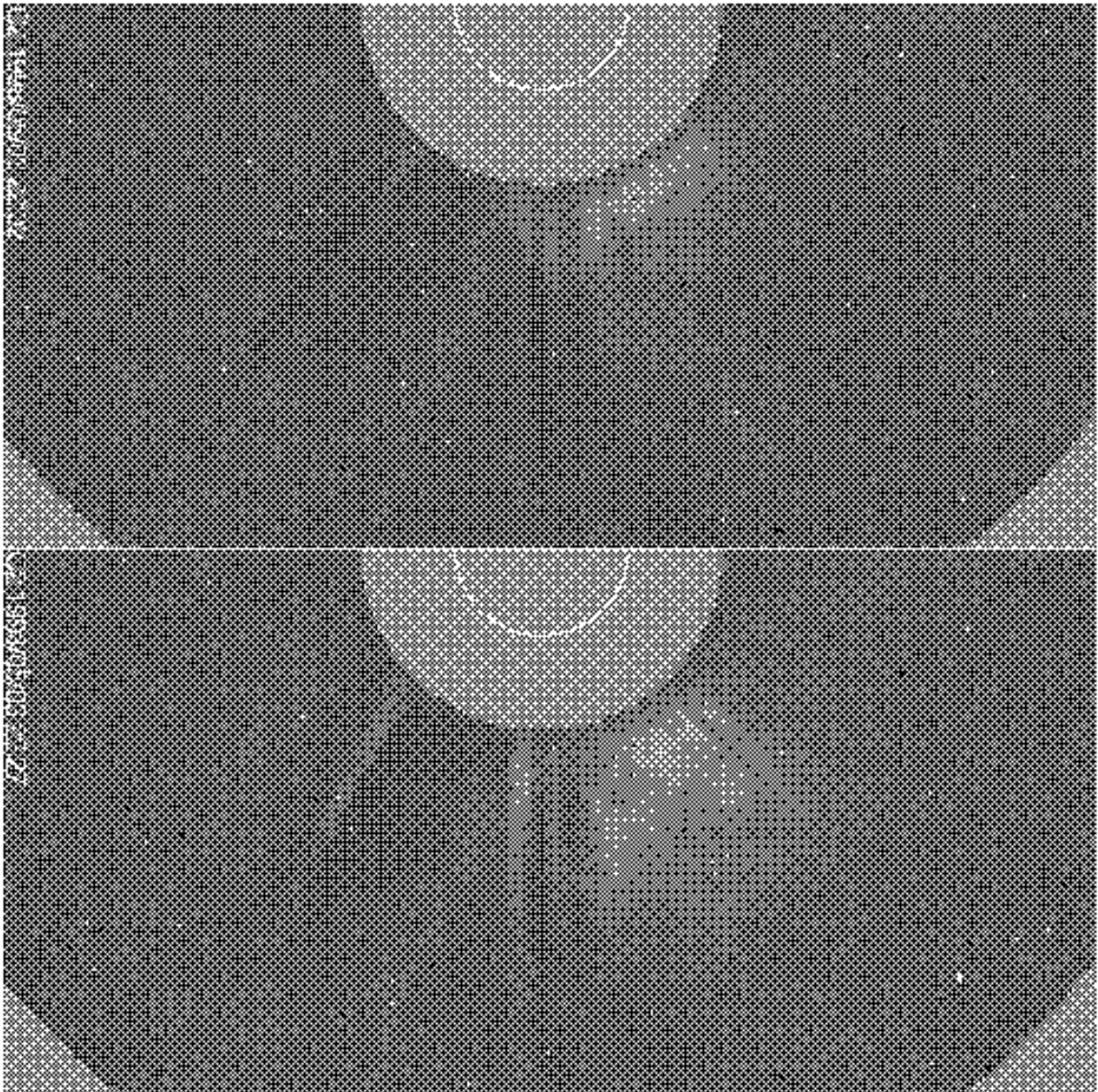


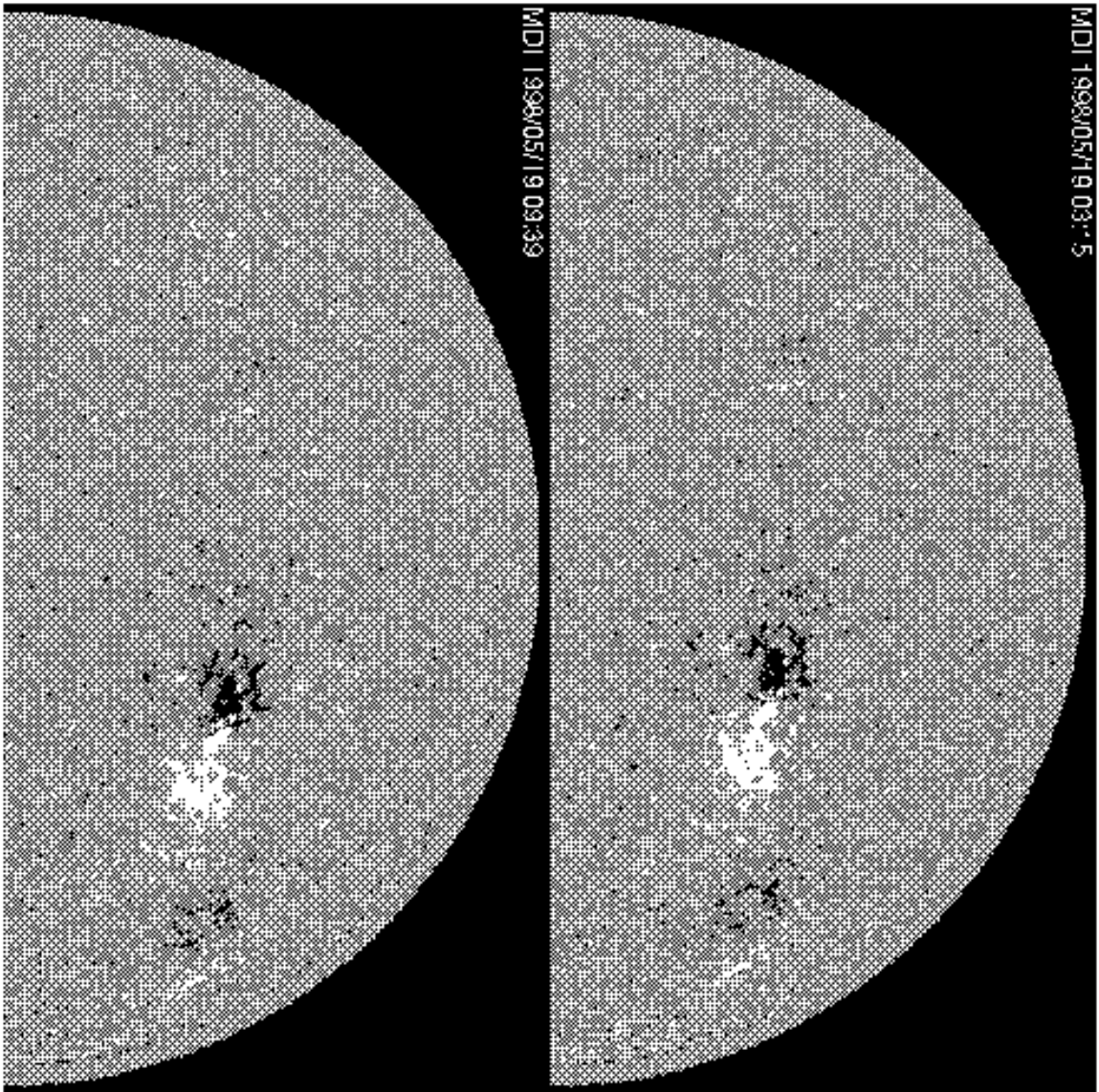












MIDI 1998/05/19 09:39

MIDI 1998/05/19 09:39



